

9-2020

Biomanufacturing Organized Collagen-Based Microfibers as a Tissue ENgineered Device (TEND) for Tendon Regeneration

Yas Maghdouri-White

Nardos Sori

Stella Petrova

Hilary Wriggers

Nathan Kemper

See next page for additional authors

Follow this and additional works at: https://digitalcommons.odu.edu/bioelectrics_pubs



Part of the [Molecular, Cellular, and Tissue Engineering Commons](#), and the [Surgery Commons](#)

Original Publication Citation

Maghdouri-White, Y., et al. (2020). Biomanufacturing organized collagen-based microfibers as a Tissue ENgineered Device (TEND) for tendon regeneration. *Biomedical Materials*. 16 (2): 1-21. Article 025025. <https://doi.org/10.1088/1748-605X/abb875>

This Article is brought to you for free and open access by the Frank Reidy Research Center for Bioelectrics at ODU Digital Commons. It has been accepted for inclusion in Bioelectrics Publications by an authorized administrator of ODU Digital Commons. For more information, please contact digitalcommons@odu.edu.

Authors

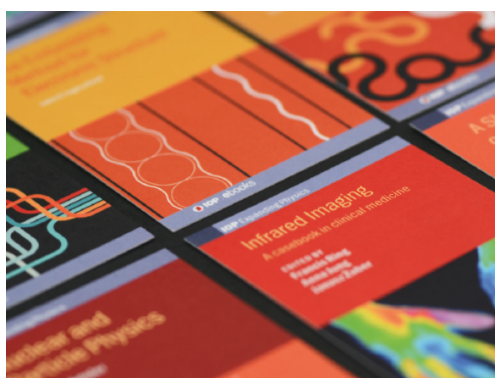
Yas Maghdouri-White; Nardos Sori; Stella Petrova; Hilary Wriggers; Nathan Kemper; Amrita Dasgupta; Kelly Coughenour; Seth Polk; Nick Thayer; Mario Rodriguez; Bill Simon; Anna Bulysheva; Kevin Bonner;; Steven Arnoczky; Samuel Adams; and Michael Francis

PAPER • OPEN ACCESS

Biomanufacturing organized collagen-based microfibers as a Tissue ENgineered Device (TEND) for tendon regeneration

To cite this article: Yas Maghdouri-White *et al* 2021 *Biomed. Mater.* **16** 025025

View the [article online](#) for updates and enhancements.



IOP | ebooks™

Bringing together innovative digital publishing with leading authors from the global scientific community.

Start exploring the collection—download the first chapter of every title for free.

Biomedical Materials



PAPER

OPEN ACCESS

RECEIVED
16 June 2020

REVISED
28 August 2020

ACCEPTED FOR PUBLICATION
14 September 2020








PUBLISHED
24 February 2021

Original content from this work may be used under the terms of the [Creative Commons Attribution 4.0 licence](https://creativecommons.org/licenses/by/4.0/).

Any further distribution of this work must maintain attribution to the author(s) and the title of the work, journal citation and DOI.



Bio manufacturing organized collagen-based microfibers as a Tissue ENgineered Device (TEND) for tendon regeneration

Yas Maghdouri-White^{1,*} , Nardos Sori^{1,*} , Stella Petrova¹ , Hilary Wriggers¹ , Nathan Kemper¹, Amrita Dasgupta¹ , Kelly Coughenour¹ , Seth Polk¹, Nick Thayer¹, Mario Rodriguez DVM², Bill Simon DPM³, Anna Bulysheva⁴, Kevin Bonner^{2,5}, Steven Arnoczky DVM⁶, Samuel Adams MD⁷ and Michael P. Francis^{1,2} 

¹ Embody Inc, Norfolk, VA 23508, United States of America

² Eastern Virginia Medical School, Norfolk, VA 23507, United States of America

³ Bayview Physicians, Atlantic Foot & Ankle Center, Virginia Beach, VA 23454, United States of America

⁴ Frank Reidy Research Center at Old Dominion University, Norfolk, VA 23508, United States of America

⁵ Jordan-Young Institute, Virginia Beach, VA 23462, United States of America

⁶ Michigan State University, East Lansing, MI 48824, United States of America

⁷ Duke University, Durham, NC 27710, United States of America

* Authors contributed equally.

E-mail: mfrancis@embody-inc.com

Keywords: bioengineered, tissue engineered, collagen, poly(D, L-lactide), tendon, TAPESTRY

Abstract

Approximately 800,000 surgical repairs are performed annually in the U.S. for debilitating injuries to ligaments and tendons of the foot, ankle, knee, wrist, elbow and shoulder, presenting a significant healthcare burden. To overcome current treatment shortcomings and advance the treatment of tendon and ligament injuries, we have developed a novel electrospun Tissue ENgineered Device (TEND), comprised of type I collagen and poly(D,L-lactide) (PDLLA) solubilized in a benign solvent, dimethyl sulfoxide (DMSO). TEND fiber alignment, diameter and porosity were engineered to enhance cell infiltration leading to promote tissue integration and functional remodeling while providing biomechanical stability. TEND rapidly adsorbs blood and platelet-rich-plasma (PRP), and gradually releases growth factors over two weeks. TEND further supported cellular alignment and upregulation of tenogenic genes from clinically relevant human stem cells within three days of culture. TEND implanted in a rabbit Achilles tendon injury model showed new *in situ* tissue generation, maturation, and remodeling of dense, regularly oriented connective tissue *in vivo*. In all, TEND's organized microfibers, biological fluid and cell compatibility, strength and biocompatibility make significant progress towards clinically translating electrospun collagen-based medical devices for improving the clinical outcomes of tendon injuries.

1. Introduction

Tendon and ligament injury and pathology present a significant burden to healthcare systems worldwide. Approximately 30 million injuries occur annually that could potentially benefit from regenerative therapeutics and tissue engineered tendon repair augmentation [1]. Although many ligament and tendon injuries may heal with satisfactory outcomes, others do not. Suboptimal outcomes resulting from soft-tissue injury, disruption and repair is often multi-factorial, however, inadequate healing response, poor tissue quality and tissue loss contributes to poor outcomes

in this group [2, 3]. In order to address these deficiencies and improve outcomes, there is likely a significant role for biological augmentation, tissue regeneration, and modification of the healing response. Implantable biologic grafts will likely be a key component to tissue augmentation and regeneration going forward in order to improve upon the current outcomes.

Autografts and allografts are often used in the repair of tendon and ligaments. Autografts have been associated with more pain and more physical limitations for up to six months when compared to allografts [4]. The leading allografts for tendon repair

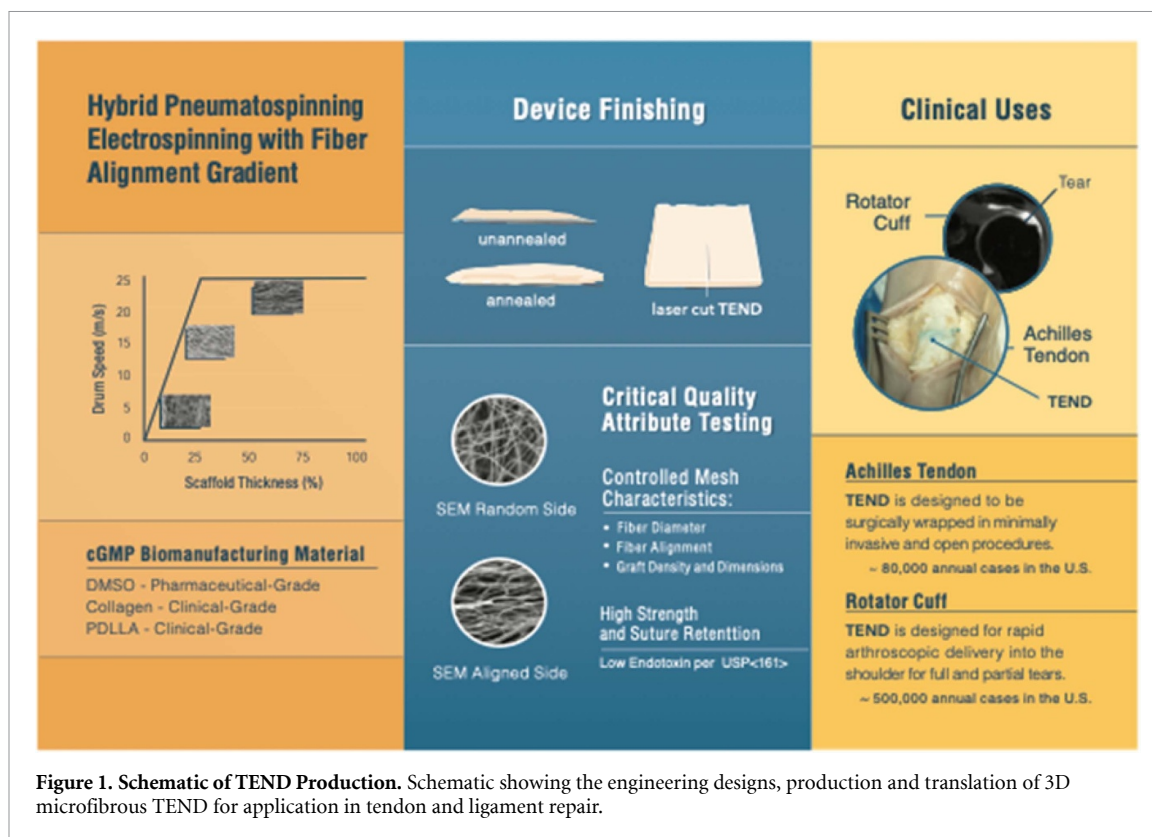


Figure 1. Schematic of TEND Production. Schematic showing the engineering designs, production and translation of 3D microfibrillar TEND for application in tendon and ligament repair.

by volume are from human cadaveric decellularized dermis [5–7]. Cadaveric dermis does not mimic the structure of the aligned extracellular matrix (ECM) arrangement or the growth factor composition of tendon tissue [8]. Moreover, cadaveric dermis was associated with chronic inflammation, poor cellular infiltration and partial material degradation [7]. Further, allografts are supply-limited, promote scar formation, may inhibit tendon healing [9], and lack clinical evidence supporting their use for tendon repair with tissue healing.

Tendons and ligaments are mainly comprised of type I collagen fibrils in an intricate, anisotropic array [8, 10]. Therefore, advanced manufacturing methods of generation of three-dimensional (3D) materials with controlled and tailorable properties are being explored. Biomanufacturing by electrospinning of microfibers is of particular interest in the field of tendon tissue engineering and may be advantageous due to its bottom-up manufacturing method, which offers capability to form materials with aligned, ordered fibrous structures that can be altered to closely mimic the structure of native tendon ECM [11–13]. Thus, biomanufacturing customized scaffolds which both replicate and regenerate tissue with anisotropic collagen patterns may be highly desirable with great potential for therapeutic use [14, 15].

Despite decades of research, to date there are no known electrospun grafts cleared by the FDA as surgical meshes for the management and augmentation of tendon injuries. Lack of clinical translation of

electrospun products for musculoskeletal and other disorders has been largely beset by poor cellular infiltration into the graft [16, 17] and limited remodeling potential of the commonly-produced electrospun graft with densely packed fibers [18]. Many potential biomaterials for musculoskeletal indications lack type I collagen [19], which is the dominant matrix material in tendons and most musculoskeletal tissues, essential for cell and growth factor attachment, and has shown to inhibit the inflammatory response common to grafts made with purely synthetic polymers [20, 21]. Thus, despite great promise, collagen-containing, electrospun grafts have not yet been commercialized, due partly to various biomanufacturing limitations.

Among the more limiting issues in scaling electrospinning for biomedical use is presence of toxic solvents [17] such as hexafluoroisopropanol (HFP), trifluoroacetic acid, and dichloromethane, commonly used to produce electrospun materials [22]. These solvents are difficult to remove from the final product [17], making most common electrospinning solvents ill-suited for clinical translation, as they have low allowable residual limits per USP <467>. In contrast, DMSO is non-toxic and has been used as a pharmacological agent for human use since at least 1978 [23]. The high dielectric constant of DMSO is favorable for fiber formation [24] and has been used in electrospinning of polymers [24–26], and collagen type I [27] as a co-solvent. However, DMSO has previously been mixed with toxic solvents such as HFP,

chloroform, and tetrahydrofuran to make it volatile to allow efficient electrospinning [24, 26]. Electrospinning from 100% DMSO is deemed important for progressing medical device translation [28] as it is non-toxic and does not completely breakdown collagen [27]. Despite enthusiasm for its use, DMSO alone has not been reported for electrospinning collagen or collagen-biopolymer blended grafts.

While collagen can be electrospun from other benign solvents [27, 29, 30], the resulting fibers are mechanically weak and unstable in aqueous solutions [27]. Many studies have demonstrated that using a biocompatible co-polymer blended with collagen offers many advantages by combining mechanical stability of the polymer and the biocompatibility of collagen [20, 31–33]. One such biopolymer used in currently marketed medical devices cleared by FDA for tendon indications is PDLA. PDLA is a combination of two optical isomers: L-lactic acid and its mirror image D-lactic acid [34] that is biocompatible, has shown to support the growth of cells, and degrades to CO₂ and H₂O (within 9–12 months) *in vivo* [35–38].

Overcoming the limits of existing grafts and technological limitations of translating additive manufacturing methods to the orthopedics and sports medicine graft biomanufacturing, the intent of this investigation was to engineer a biocompatible microfibrillar construct composed of collagen type I and ultrahigh molecular weight PDLA electrospun from DMSO and to determine its ability to support connective tissue regeneration. We hypothesize that the fiber alignment and porosity of this Tissue Engineered Device (TEND) will promote rapid cell infiltration and alignment as well as induction, maturation, and remodeling of host tissue in an *in vivo* tendon injury model. Additionally, we hypothesize that the novel design of TEND will act as a carrier for bioactive products such as platelet-rich-plasma (PRP) and mesenchymal stem cells, further potentiating its biomimetic activity and serve as a delivery vehicle for biologics of interest for clinical use in tendon, ligament and other soft-tissue surgical repairs (figure 1).

2. Materials and methods

2.1. Electrospinning setup

Aligned TEND was produced by dissolving type I collagen (Collagen Solutions, Eden Prairie, MN) and UHMW PDLA (Corbion, Amsterdam, Netherlands) in 100% DMSO (Gaylord Chemical, Slidell, LA) at a final concentration of 100 mg ml⁻¹ (30 mg ml⁻¹ collagen and 70 mg ml⁻¹ PDLA) for 24 h. This polymer blend was electrospun onto a spoked-wheel collector in a vertical electrospinning setup. Evaporating the nonvolatile DMSO was accomplished by a hybrid form of electrospinning and pneumatospinning [39], providing constant

pressure laminar airflow from a fan at the emitter directed towards the collector, and exhausting the air from directly above the collector. The surface speed of the drum was 18 m s⁻¹. The distance between the needle and the collecting drum was 130 mm. A 25-gauge needle was used, and the solution flow rate was set to 1 ml hr⁻¹. Humidity was maintained between 45%–50% and temperature was between 23 °C–26 °C. Upon completion of the electrospinning process, TEND was removed and placed under vacuum for 24 h at ambient temperature to aid with removal of any residual DMSO. Throughout this manuscript term ‘TEND’ has been used to address all electrospun grafts in general. Term ‘as-electrospun TEND’ is used when this condition is compared to the annealed TEND as explained in section 2.2.

2.2. Post-processing of TEND by annealing

Most electrospun materials significantly shrink due to thermally induced relaxation of stretched amorphous chains [40]. However, thermal annealing of many polymers [41–44] has led to improvements in their mechanical stability by changing microstructural properties and their degree of crystallinity. Here, as-electrospun TEND was gripped in aluminum frames and held under tension during post-processing. The framed sheets were annealed under vacuum at various temperatures and durations for optimization. TEND annealed at 65 °C for 18 h demonstrated highest degree of stability compared to all the temperatures and durations tested, therefore, for the remainder of experiments all TEND were annealed under these conditions. Throughout this manuscript the electrospun grafts that have been annealed are referred to as ‘annealed TEND’.

2.3. Scanning electron microscopy (SEM)

SEM was performed at Jefferson Labs (Newport News, VA) using a JEOL JSM-6060 LV microscope (JEOL Ltd., Tokyo, Japan) with a 20 kV beam intensity. The SEM images were analyzed with ImageJ software (NIH Shareware, Bethesda, MD) to determine fiber diameter and fiber alignment of annealed and as-electrospun TEND at day 0 and after a 14-day incubation in Dulbecco’s modified eagle medium (DMEM) at 37 °C with 5% CO₂.

2.4. Sodium dodecyl sulfate polyacrylamide gel electrophoresis (SDS-PAGE)

SDS-PAGE was comparatively used to identify the alpha I and II chains present in monomeric triple helical collagen feedstock (Collagen Solutions), and in annealed and as-electrospun TEND. Samples were run on NuPAGE 3%–8% tris-acetate gels at 150kV on PowerEase 300 W. The gel was removed and stained with SimplyBlue gel stain for 1 h and then rinsed with deionized water for 1 h. All items were from Thermo Fisher Scientific.

2.5. Fourier transform infrared spectroscopy (FTIR)

FTIR was performed on Platinum ATR (Brucker, Billerica, MA) at Old Dominion University (ODU) (Norfolk, VA) to confirm the presence of the three amide bonds characteristic of type I collagen at 1235, 1560, and 1650 nm wavelengths. Bond peaks of electrospun and annealed TEND were compared to collagen and PDLA feedstocks.

2.6. Gas chromatography mass spectrometry (GCMS)

Mass spectrometry was used to analyze the presence of DMSO in TEND after 0, 2, 4, 6, and 24 h under vacuum. After vacuum, approximately 20 mg of test material was suspended in 3 ml of Dimethylacetamide and heated to 60 °C with agitation for 24 h. Supernatants were collected for GCMS analysis. Replicate extracts were prepared for each sample. A second extraction was conducted to confirm complete recovery of residual DMSO. The extracts were run on Agilent 7890 A GC. The GCMS testing was performed by InVision Biomedical Group, Inc. (Irvine, CA).

2.7. Thermogravimetric analysis (TGA)

TGA analysis was performed to assess the presence of residual DMSO within TEND. TGA data of as-electrospun TEND samples placed under vacuum for 0 and 24 h was obtained from a TGA Q5000 (TA instruments, New Castle, DE) at ODU. Data was collected at a rate of 5 °C min⁻¹ from 21 °C to 300 °C.

2.8. Porosity/void measurements

Mercury intrusion porosimetry was performed at Quantachrome Instruments (subsidiary of Anton Paar, Boynton Beach, FL) on triplicate samples of as-electrospun and annealed TEND on a PoreMaster 60, with analyses performed blinded to sample identity. Gas sorption was also performed at Quantachrome on triplicate samples of as-electrospun or annealed TEND on an AutoSorb IQ, with analyses performed blinded to sample identity, including calculation of mean Brunauer–Emmett–Teller (BET) surface area.

2.9. Sterilization

TEND used for these studies were cut into the required sizes and inserted into Tyvek pouches (4MD Medical Solutions, Lakewood, NJ). Tyvek pouches were sealed with a heat sealer and sent for electron beam sterilization (Steri-Tek, Fremont, CA) using a 20 ± 2kGy target dose. Mechanical testing and chemical characterization of TEND were performed before e-beam sterilization.

2.10. Mechanical stability of TEND in culture

E-beam sterilized as-electrospun and annealed TEND were incubated in DMEM with 1% antibiotic-antimycotic (ABAM) (Thermo Fisher Scientific, San Diego, CA) at 37 °C with 5% CO₂ for seven

days. After seven days, their mechanical properties were tested by uniaxial tensioning in the direction of aligned fibers at room temperature using an MTS Criterion Model 42 (Eden Prairie, MN) at a rate of 1 mm s⁻¹. As-electrospun and annealed TEND soaked in Dulbecco's phosphate buffered saline (DPBS) (Fisher Scientific, Hampton, NH) for 30 min were used as Day 0 controls. The dimensions of the samples at day 0 and day 7 were used to calculate the percentage of material shrinkage. The fiber diameters assessed using SEM images were used to calculate percentage of material swelling.

2.11. Blood absorption

Human blood with anticoagulant heparin and citrate dextrose (ACD-A) was purchased from Biological Specialty Corporation (Colmar, PA). A calcium chloride (CaCl₂) (Fisher Scientific) concentration of 1.25% was found required to initiate coagulation in clotting blood supplemented with ACD-A. Annealed TEND samples (40 × 40 × 1 mm) were immersed in clotting blood (ACD-A + CaCl₂) and heparinized, non-clotting blood. Soaked samples were weighed in intervals of 5 min to calculate the amount of blood absorbed. Volume of absorbed blood was calculated by using density of 1 ml of blood. Dimensional changes after blood hydration was calculated by snap freezing the samples in liquid nitrogen and measuring the size using calipers (*n* = 3). Samples immersed in blood as above and in a fresh draw from a rabbit ear vein were fixed in 2.5% glutaraldehyde in 0.1 M Sodium cacodylate buffer, pH 7.4 (Electron Microscopy Sciences, Hatfield, PA) at 4 °C. Fixed samples were washed with 3X phosphate buffered saline (PBS) (Thermo Fisher Scientific) for ten minutes, placed in 100% hexamethyldisilazane (HMDS) (Electron Microscopy Sciences, Hatfield, PA) for 3 min, and then air dried. Samples were further imaged by SEM.

2.12. PRP activation and lysate isolation

Human PRP with anticoagulant citrate dextrose (ACD-A) (ZenBio, Research Triangle Park, NC) was stored at 4 °C for 30 min, then calcium chloride (CaCl₂) (Fisher Scientific) was added to reach a final concentration of 22 mM. The PRP solution was mixed and placed at 37 °C for 1 h to activate. After clotting, the lysate was collected for use on annealed TEND. Annealed TEND (10 × 10 mm) (*n* = 4) and size-matched rabbit Achilles tendon (*n* = 4) were soaked in 1 ml of PRP lysate for 6 min followed by placement in 600 μl of modified eagle medium (MEM) (Fisher Scientific) with 2% ABAM. Negative controls consisted of annealed TEND soaked for 6 min in MEM with 2% ABAM only. Samples were incubated at 37 °C with 5% CO₂. After 30 min, 4, 8, 24 h, and 3, 7 and 14 d, MEM was collected from each well and stored at -80 °C. MEM was replenished after each time point.

2.13. Enzyme linked immunoabsorbent assay (ELISA)

TENDS's binding and release of growth factors typically found in high concentrations in PRP was assessed using ELISA's specific for TGF- β 1 and PDGF-BB (R&D Systems, Minneapolis, MN and RayBiotech, Norcross, GA). The elution kinetics of TGF- β 1 and PDGF-BB from the electrospun grafts and native tissue was assessed per the manufacturer's instructions at the timepoints per section 2.12.

2.14. Mechanical properties of PRP coated TEND

Two sets of annealed TEND were cut into 10×30 mm ($n = 6$ per group). One set of samples were soaked in PRP for 10 min. PRP soaked TEND and a second set of non-coated TEND were placed in grips under static tension and remained in culture at 37 °C and 5% CO₂ for up to seven days. The samples were removed from the grips after 3 and 7 d in culture and their mechanical properties were tested at room temperature by uniaxial tensioning in the direction of aligned fibers using an MTS Criterion Model 42 at a rate of 1 mm s^{-1} . Annealed TEND soaked in DPBS (Fisher Scientific) for 30 min were used as Day 0 controls.

2.15. Cell culture

Human tenocytes (ZenBio) were cultured in tenocyte culture medium (ZenBio). Human bone marrow-derived MSCs (RoosterBio[®], Ballenger Creek, MD) were cultured and maintained in serum-free, xeno-free media (RoosterBio[®]). All cell cultures were maintained under physiological conditions at 37 °C and 5% CO₂.

2.16. Cell viability, morphology and infiltration

To assess human tenocyte cell proliferation on TEND, one set of each as-electrospun or annealed gripped TEND (10×30 mm) ($n = 6$) and one set of each as-electrospun or annealed loose TEND (10×30 mm) ($n = 3$) were seeded with 2.5×10^4 human tenocytes per TEND to allow sufficient surface area for cell growth over the course of two weeks. Cellular activity was assessed after 1, 7 and 14 d in culture. The alamarBlue[®] metabolic activity assay (Bio-Rad) was used per the manufacturer's protocol to test cellular viability and proliferation. Cell infiltration and morphology was assessed over 14 d in culture. One set of each as-electrospun or annealed gripped TEND ($n = 3$) and one set of each as-electrospun or annealed loose TEND ($n = 3$) were seeded with 1×10^5 cells/construct. Cellular infiltration was assessed after 1, 7 and 14 d in culture. Cells were fixed in 4% paraformaldehyde and stained with 4',6-diamidino-2-phenylindole (DAPI) (Fisher Scientific) nucleic stain. Cellular infiltration from the surface of TEND was measured with a Zeiss Axio Observer Z1 confocal microscope (Zeiss, Oberkochen, Germany). Five fields of view per TEND were investigated. At each field of view, multiple 5 μ m

thick z-scan slices were captured, and the total depth of cell infiltration was calculated based on the number of cell-containing slices captured. The total depth was averaged for the five fields of view. To visualize cell morphology and elongation, all TEND cultured with human tenocytes were fixed in 4% paraformaldehyde and stained for nuclei and actin filaments using DAPI nucleic stain and Alexa Fluor[®] 594 phalloidin (Thermo Fisher Scientific), respectively. The stained samples were imaged using a Zeiss Axio Observer Z1 confocal microscope. Percentage of cell elongation was determined based on the average calculated nuclei aspect ratio by measuring the length and width of twenty cell nuclei using ImageJ FIJI (NIH Shareware). Measurements were performed using confocal images taken at 40X magnification.

2.17. Mechanical testing of cellularized and acellular annealed TEND

To compare mechanical stability of acellular and cellularized TEND, one set of each ($n = 12$) was placed in custom grips and held under static tension (gripped) to prevent shrinkage and promote further fiber alignment. A second set of annealed TEND ($n = 12$) was placed in ultra-low cell binding culture plates without tension (loose). Half of each set of TEND, gripped ($n = 6$) or loose ($n = 6$), were seeded with 1×10^5 human tenocytes per side for a total of 2×10^5 cells per TEND. All samples remained in culture for 7 and 14 d. At each time point, the samples were removed from the wells and pulled to failure under uniaxial tension in the direction of the aligned fibers. Annealed TEND at day 0 (controls) were hydrated in DPBS for 30 min prior to testing. All samples, cellularized and acellular, were mechanically tested at room temperature using an MTS Criterion Model 42 (Eden Prairie, MN) at a rate of 1 mm s^{-1} . Thickness was measured with a Mitutoyo 547–526 S (Takatsuku, Kawasaki, Japan) thickness gauge.

2.18. Bioreactor culture

Annealed TEND ($n = 6$) were pre-coated with human PRP for 10 min. Clinical grade mesenchymal stem cells derived from human bone marrow (RoosterBio[®]) were seeded on the PRP coated TEND at 5×10^5 cells/TEND. One half of the constructs ($n = 3$) were placed in a custom designed cyclic-loading bioreactor. The spring-driven load on the bioreactor had a spring constant of 0.125 N mm^{-1} and was cycled between 0 and 8 mm resulting in a 0–1 N sinusoidal wave. The bioreactor chamber contains 316 stainless steel, polyether ether ketone (PEEK) and medical grade silicone. The polycarbonate window provided two ports for gas exchange. A second set of cell seeded constructs ($n = 3$) were placed in static grips and kept under static tension. Cultures were maintained with defined media for three days prior to qPCR analysis.

2.19. Quantitative PCR

RNA extraction was performed by pooling $n = 2$ or 3 individual TEND samples and lysing the cells within TEND directly in complete lysis buffer from the RNEASY Plus mini prep kit (Qiagen, Valencia, CA). TEND samples were cut into small pieces and then vortexed vigorously for 10 min. RNA was extracted following the manufacturer's protocol. The amount of RNA extracted was measured using a NanoDrop spectrophotometer. Up to 750 ng of total RNA was converted to cDNA using the protocol described in the SuperScript™ III First-Strand Synthesis SuperMix kit (Life Technologies, Grand Island, NY). 40–50 ng of cDNA was used in qPCR reactions following the manufacturer's protocol for the SoFast™ Evagreen® Supermix (Bio-Rad, Hercules, CA) and primers specific to the target human genes were obtained from published references [45–50]. Reactions were run in triplicates on the CFX Connect™ Real-Time PCR Detection System (Bio-Rad) on 96 well plates, using 39 cycles with an annealing temperature of 56 °C. A single amplicon product was confirmed by the detection of a single peak on the melt curve. mRNA transcript levels were normalized to corresponding glyceraldehyde-3-phosphate dehydrogenase (GAPDH) values. Results were consolidated and analyzed using the instrument's supporting software (CFX Maestro Software, BioRad).

2.20. Rat surgical implantation

All surgical procedures were conducted according to a protocol approved by Institutional Animal Care and Use Committee (IACUC), Old Dominion University. Per ISO 10 993–6, $n = 6$ grafts of TEND and allograft dermis (Wright Medical, Memphis, TN) were implanted for 2, 4, 8 and 16-weeks in a pool of male and female Sprague Dawley rats. Rats were anesthetized with isoflurane inhalation. Flanks were shaved, and Nair depilatory cream was applied to remove hair from the surgical site. Incisions were made dorsally in the flank area and a hemostat was used to create a pocket for implants. Once grafts were implanted in the pocket, the incision was closed using suture. After the designated time points, the rats were humanely euthanized for tissue collection.

2.21. Rabbit surgical implantation

All surgical procedures were conducted according to a protocol developed based on studies by Van Kampen *et al* [51] and approved by Institutional Animal Care and Use Committee (IACUC), Eastern Virginia Medical School. TEND grafts were implanted for 4, 16 and 52-weeks in the Achilles tendon of male New Zealand White Rabbits and compared with sham (suture alone). Rabbits were administered with Acepromazine and anesthesia induced using isoflurane. Clippers and Nair depilatory cream were used to remove hair from hind legs. Surgical sites

were cleaned and aseptically prepared with alternating passes of betadine and 70% alcohol. The calcaneal tendon was exposed through paratendineal incision of the cutis, subcutis and fascia. Using a number 10 scalpel blade, three full thickness incisions (1 incision per bundle) approximately 7 mm long were made in the coronal plane of the calcaneal-Achilles tendon, midsubstance between the calcaneus and the gastrocnemius. Annealed TEND was circumferentially placed around the Achilles tendon defects (similar to the implantation in the cadaver model shown in figure 12) and sutured into place using 4–0 Mersilene®. The peritenon was closed using 4–0 Vicryl® suture. The incision site was closed with a 4–0 Vicryl® running suture. For sham, sutures were placed in identical pattern as the graft using 4–0 Mersilene® and 4–0 Vicryl® to close the peritenon. After surgery, antibiotic was placed on the incisions and the operated legs wrapped with surgical gauze and cotton roll. Vet wrap was used to wrap the leg and hold it in place. Surgical gauze, cotton roll and Vet wrap were removed after 24 h. Animals were fed using a food hopper from inside the cage after surgery. The rabbits were not allowed outside of their cages for 14 d post-op in order to restrict their movements to ensure proper healing of the defect. At the endpoint, the animals were euthanized by deep anesthesia with isoflurane inhalation followed by barbiturate overdose (1cc per 10 pounds) with confirmation of death with a bilateral thoracotomy.

2.22. Histology

Harvested graft explants were fixed in 4% paraformaldehyde (Alfa Aesar, Haverhill, MA) for 24 h then transferred to PBS. Samples were sectioned to 5 µm thickness and serial sections were stained with Masson's trichrome and H&E at IDEXX (West Sacramento, CA). QuPath, an open source software, was used to quantify the number of cells on the histology sections. Three H&E slides of each graft types were chosen, and images taken using 10X magnification. A representative image of the graft from each slide was selected to run on QuPath. Polarized light microscopy was used to image newly produced collagen within TEND implants and sham controls. The alignment of the deposited collagen was assessed using Directionality function of ImageJ software.

2.23. Cadaver surgical implantation

Cadaveric implantation was performed in the prone position through a posterior transverse 3-centimeter incision at a level 4–6 centimeters from the superior margin of the calcaneus. The Deep Fascia and Paratenon were incised and maintained for later closure. An irregular cut was made full thickness through the Achilles tendon to mimic a clinical rupture. A minimally invasive repair technique was performed with a suture passer using suture tape passed along each side of the proximal tendon to the level of the rupture.

The suture was then passed through the distal tendon rupture using a suture retriever, passed through a transverse bone tunnel in the calcaneus, tensioned to bring the ruptured ends together and tied with a surgeon's knot. TEND was then properly oriented and passed via the plastic inserter under and around the Achilles tendon repair site. It was fixated with standard 3–0 Vicryl suture to the host tendon. A 22-gauge needle was used to make multiple passes through TEND and into the Achilles tendon to mimic the use of PRP injection augmentation. The Paratenon and Deep Fascia was closed with 3–0 Vicryl. Skin was sutured with 3–0 Nylon. The ankle was then taken through a range of motion to check the integrity of the repair with TEND in place. Inspection of the repair and TEND was then performed by careful dissection of the surrounding skin and subcutaneous tissue.

2.24. Statistics

Data analysis was performed on Prism 8 software. All parameters are expressed as mean \pm S.E.M. Two-way ANOVA followed by the post-hoc Tukey's Multiple Comparison Test and Unpaired t tests were used to assess the differences in mechanical properties and fiber diameters. The Kolmogorov-Smirnov test was used to assess the differences in TEND fiber alignment and newly formed collagen alignment *in vivo*. Paired t test was used to assess the differences in PRP release kinetics. The chi-square test was used to assess the differences in frequency distribution of cellular alignment. Two-way ANOVA followed by the post-hoc Tukey's Multiple Comparison Test was used to assess the differences in *in vitro* cell elongation, cell attachment, proliferation, and infiltration, mechanical properties of the cellularized and acellular TEND, and cell quantification of rat subcutaneous implants. An unpaired t-test and ordinary one-way ANOVA followed by the post-hoc Dunnett's Multiple Comparison Test was used to assess the differences in gene expression. *A priori*, p values below 0.05 were defined as significant in all studies.

3. Results

3.1. Physical and mechanical properties of annealed and as-electrospun TEND

Hybrid pneumatospinning—electrospinning setup allowed manufacturing of highly aligned collagen:PDLLA fibrous grafts from 100% DMSO. The resulting as-electrospun TEND exhibit an average peak stress of 13.6 ± 0.26 MPa, modulus of 152.2 ± 15.85 MPa, and could withstand 8.4 ± 1.77 N load. In order to improve the porosity and void fraction of TEND, as-electrospun TEND were heated above their glass transition temperature for annealing. As demonstrated in figures 2(A) and (B), the annealing process caused TEND to expand in thickness, hence increasing the void fraction within the construct. The physical and mechanical properties

of annealed and as-electrospun TEND were tested in culture and compared to assess the effects of annealing. The structure and alignment of both as-electrospun and annealed TEND at day 0 and 14 d in culture are shown in figures 2(C)–(F). Annealing under tension resulted in significantly smaller fiber diameters ($p < 0.01$) and higher degree of fiber alignment ($p < 0.05$) compared to as-electrospun TEND at day 0 or after 14 d in culture (figures 2(G) and (H)). The higher degree of loss of fiber alignment resulting in formation of disorganized fibers in as-electrospun TEND after remaining in culture is due to shrinkage of TEND. It was demonstrated that annealing resulted in significantly smaller amount of TEND shrinkage in culture compared to as-electrospun TEND (figure 2(I)). Uniaxial tensile testing of TEND revealed that there was no significant difference in the peak stress and modulus of annealed and as-electrospun TEND at day 0 (figures 2(J) and (K)). Although both annealed and as-electrospun TEND exhibited a significant decrease in their peak stress and modulus after 7 d in culture, it was shown that annealed TEND retained significantly higher peak stress (2X higher) and modulus (11x higher) compared to as-electrospun TEND (figures 2(J) and (K)). Furthermore, at day 7 there was no significant decrease in the load bearing capability of TEND compared to Day 0 (figure 2(L)). Day 0 samples used for mechanical testing were pre e-beam sterilization, however TEND tested post sterilization exhibited no significant difference in its mechanical properties (Data not shown). Since annealing significantly increased the thickness of as-electrospun TEND, we tested if the internal void fraction of TEND was altered pre- vs. post-processing. Mercury intrusion porosimetry analysis showed that annealing process increases the average pore size of aligned fibers from $7.1 \mu\text{m}$ to $100.7 \mu\text{m}$ (figure 2(M)). Gas sorption showed that annealed TEND's 'pore' structure throughout the graft was large slit-shaped, per the adsorption-desorption hysteresis curves (figure 2(N)). Additionally, annealing increased the graft surface area significantly, as validated by gas adsorption methods (figure 2(O)).

3.2. Chemical analyses of TEND

SDS-PAGE gel electrophoresis was used to examine the impact of electrospinning and heat on collagen protein in TEND. Collagen starting material and annealed TEND were dissolved in acetic acid and run on a gel (figure 3(A)). Distinct bands visible around 238kD and 117kD confirm the presence of alpha and beta regions, respectively within TEND. Moreover, lack of smearing or laddering below 117kD showed collagen did not molecularly breakdown due to manufacturing. The difference in band intensity between collagen raw material and annealed TEND is due to different amounts of collagen loaded as the raw material is 100% collagen and the same

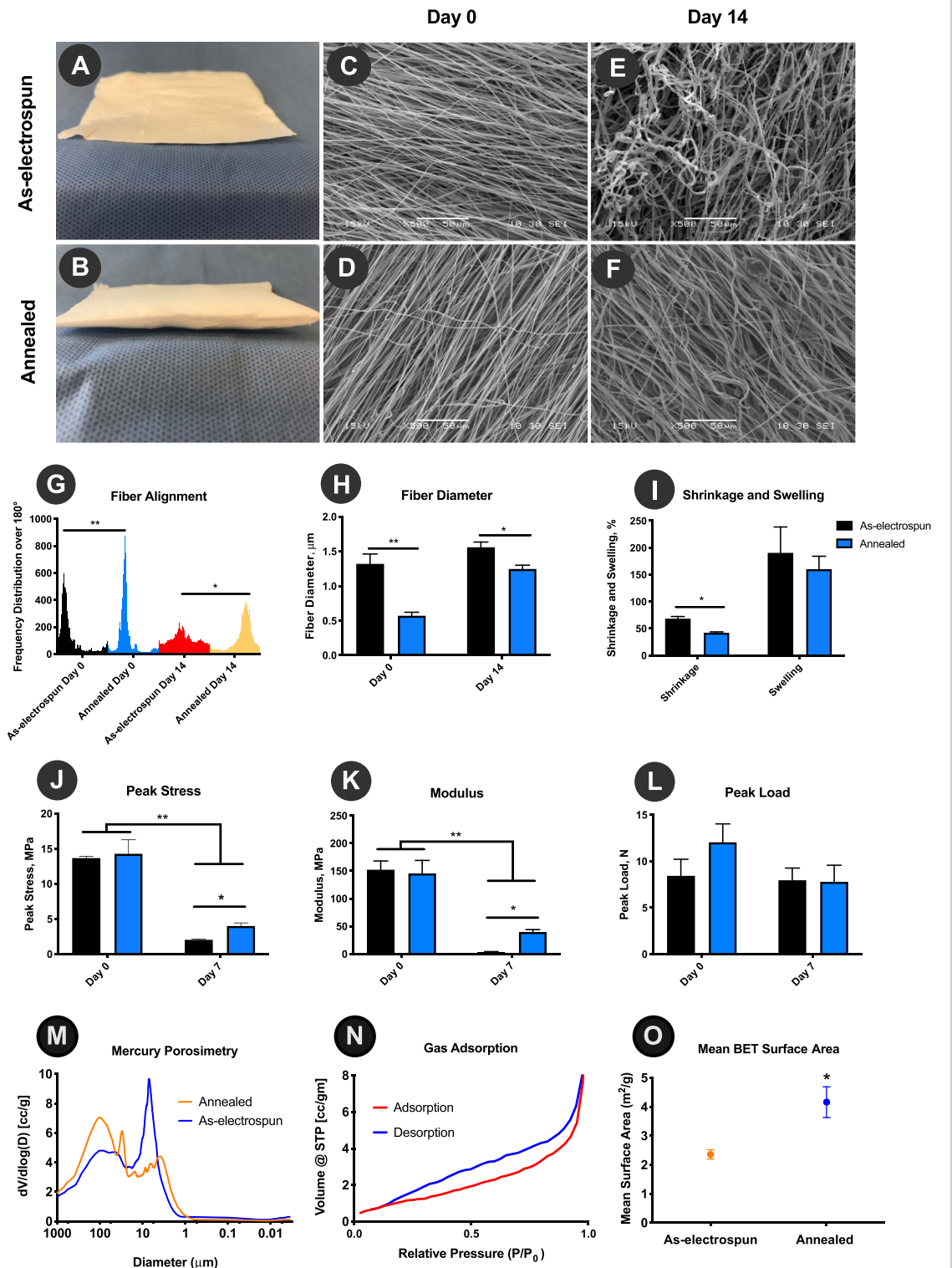
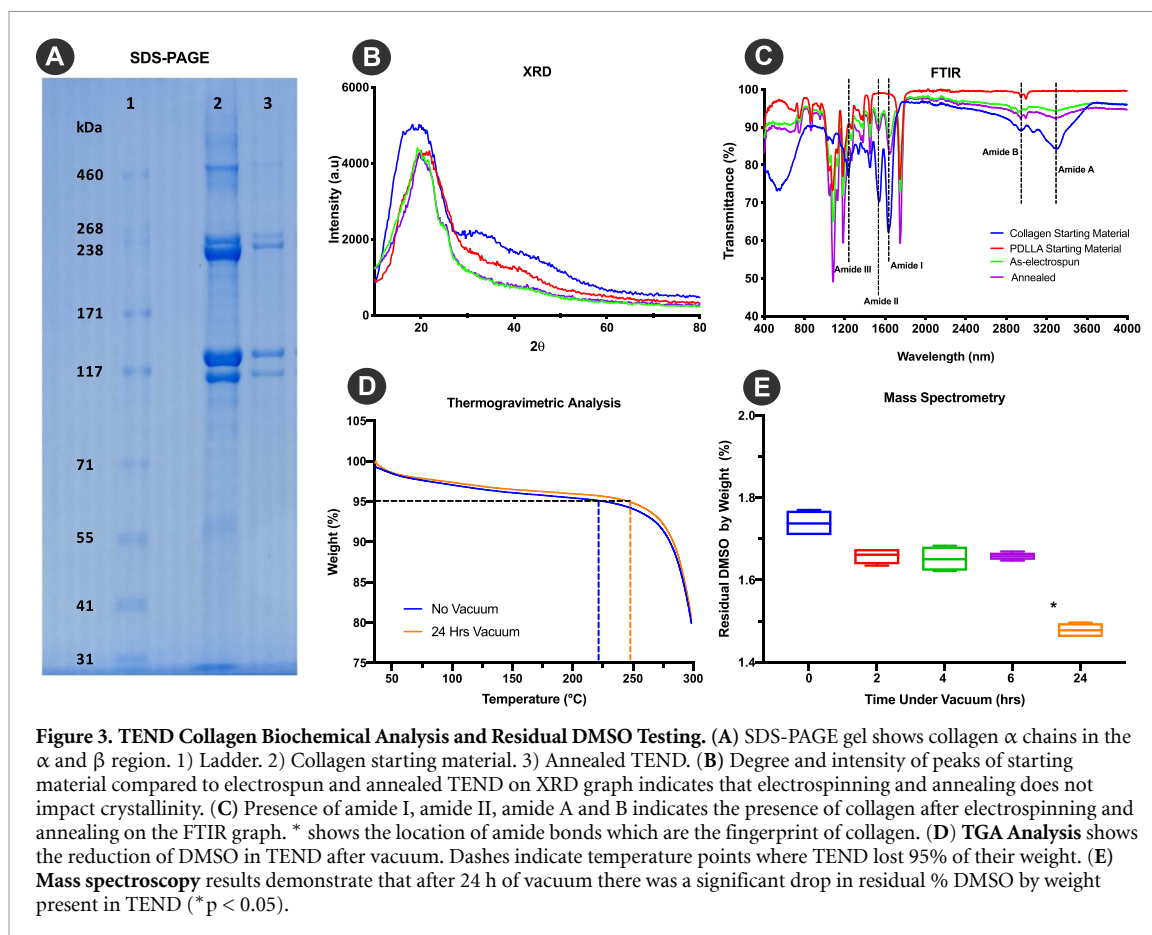


Figure 2. Annealing Significantly Enhances Physical and Mechanical Properties of TEND. As-electrospun TEND restrained in frames were heated above their glass transition temperature to promote molecular alignment and improve stability. The annealing process resulted in formation of thicker constructs (B) with improved fiber alignment (D), which retained their fiber orientation after 14 d in culture (F). (G) and (H) **Fiber Alignment and Diameter**, annealed TEND exhibited significantly smaller fiber diameters and higher degree of fiber alignment at day 0 and after 14 d in culture (** $p < 0.01$ and * $p < 0.05$) compared to as-electrospun TEND, which lost their aligned fiber orientation and became highly disorganized. (I) **Shrinkage and Swelling**, annealed TEND exhibited significantly smaller amount of shrinkage after 7 d in culture ($p < 0.05$). (J) and (K) **Peak stress and Modulus**, After 7 d in culture annealed TEND exhibited significantly higher peak stress and modulus ($p < 0.05$). (L) **Peak Load**, there were no significant differences in the peak load between annealed and electrospun TEND at day 0 or after 7 d in culture ($p > 0.05$). (M) **Changes in TEND Porosity**, As-electrospun TEND had an average pore size of 7.1 μm compared to the average pore size in annealed TEND at 100.7 μm , as assessed by mercury intrusion porosimetry. (N) **Gas Adsorption** of annealed TEND revealed large slit-like channels present throughout annealed TEND, with (O) **mean BET surface area** shown to be significantly increased in the annealed electrospun TEND compared to conventionally electrospun scaffolds.



amount of TEND in weight only contains 30% collagen. The lower band intensity due to smaller amount of collagen is not suggestive of denaturation into gelatin, as alpha, beta and gamma chains are all present in TEND as in the starting material, while there is no laddering effect that migrates faster than the alpha chain. TEND fiber crystallinity assessed by XRD showed collagen feedstock with a broad peak at approximately 20 degrees, as seen in as-electrospun and annealed TEND with a sharper peak within the same region (figure 3(B)), indicating that TEND maintained collagen crystallinity post-processing. FTIR results indicate that as-electrospun and annealed TEND had amide I (~ 1650 cm^{-1}) and amide II (~ 1560 cm^{-1}) which are the fingerprints of collagen, as well as amide A (~ 3285 cm^{-1}) and amide B (~ 2917 cm^{-1}) (figure 3(C)). The presence of amides I, II, A, and B confirmed collagen presence in TEND post-annealing. TGA was run on as-electrospun TEND before and after vacuuming. After 24 h under vacuum, 95% of the weight lost is closer to 250 $^{\circ}\text{C}$ rather than with negligible loss at 189 $^{\circ}\text{C}$, the boiling point for DMSO (figure 3(D)), indicating DMSO was removed during the manufacturing process. Removal of DMSO was further confirmed by mass spectrometer. GCMS results indicate that after 24 h of vacuum, average percent by weight of DMSO in TEND dropped from 1.74% to 1.48% (figure 3(E)) which is $> 1/1000$ th of the 50 mg day^{-1} allowed in

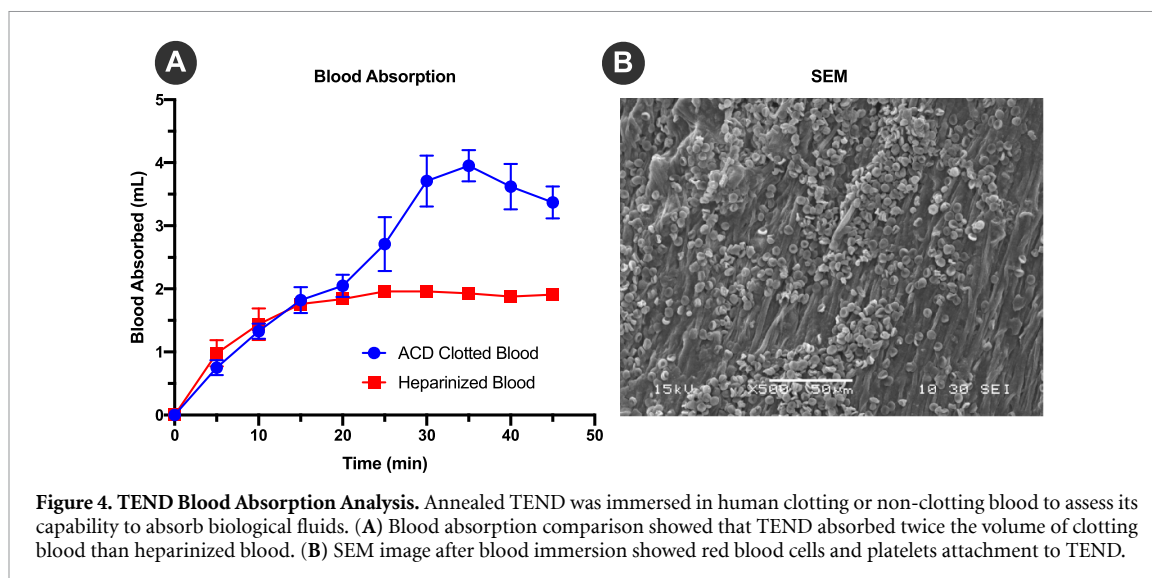
an implant per USP $< 467 >$. SDS-PAGE of TEND post e-beam sterilization also showed the presence of collagen α chains (Data not shown).

3.3. TEND blood absorption

As patient blood is commonly drawn for preconditioning surgical implants and may be either heparinized or non-heparinized, the blood absorption capability of TEND was measured by soaking in clotting blood and comparing it to heparinized blood. After 35 min on average, TEND soaked in clotting blood absorbed more than twice the volume (3.95 ± 0.43 ml) compared to TEND soaked with heparinized blood (1.93 ± 0.12 ml) (figure 4(A)). After soaking in blood for 45 min, the length, width and thickness of each sample was measured. The percent change in volume between the heparinized and clotting blood-soaked TEND were found to be insignificant ($p > 0.05$). SEM images of the human blood-soaked TEND showed red blood cell and platelet attachment on the samples (figure 4(B)).

3.4. Growth factor release kinetics and mechanical properties of PRP coated TEND

The PRP release kinetics results demonstrated that annealed TEND sequester and controllably release PRP over 14 d, as measured by release of PDGF-BB and TGF β 1 (figures 5(A) and (B)). Overall, TEND binds and releases significantly higher amounts of



PRP-derived growth factors compared to native tendon (figures 5(A) and (B)). Moreover, TEND coated in PRP and incubated under static tension exhibit improved mechanical stability and tensile strength in culture demonstrated by significantly higher peak stress and modulus (figures 5(C) and (D)) as related to changes in graft thickness in PRP. There were no significant differences observed in peak load over time (figure 5(E)), showing high graft stability upon use. Additionally, PRP-coated TEND exhibited lower strain at break than non-coated TEND, although this difference was significant only at the 3-day time point. The lower strain at break within the PRP-coated TEND is representative of the increase in modulus (** $p < 0.01$) (figure 5(F)).

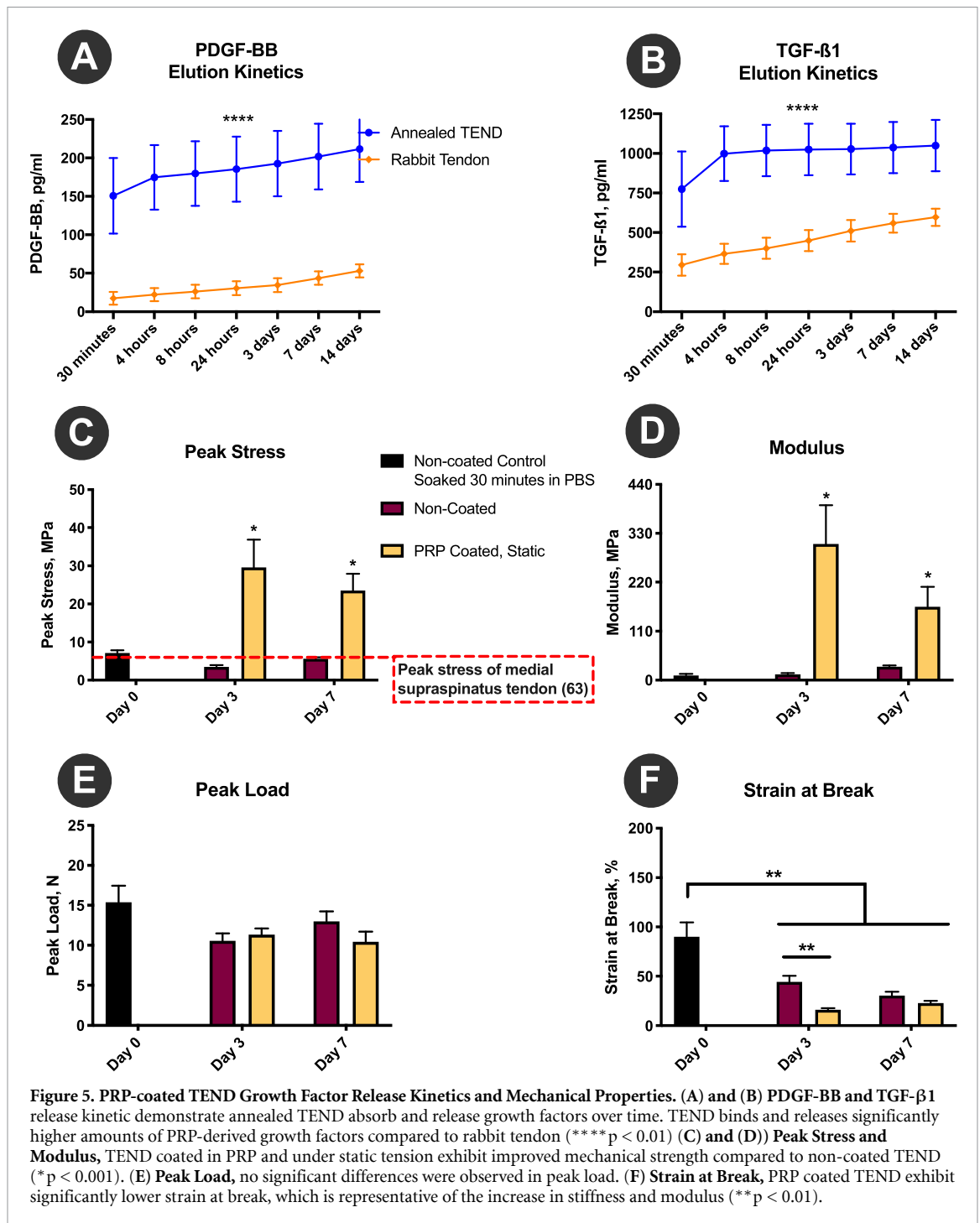
3.5. Cytocompatibility, cellular morphology and elongation

Cellular morphology and elongation of human tenocytes on as-electrospun or annealed TEND were assessed. The direction of actin filaments (red), shown in the confocal images (figures 6(A)-a and (A)-b) demonstrated cell elongation on the gripped annealed and gripped as-electrospun TEND along the direction of the fibers (figures 6(A)-e and (A)-f). The random morphology of actin filaments in the cells on loose TEND (figures 6(A)-c and (A)-d) demonstrated the loss of fiber alignment within these constructs. This random morphology is confirmed by SEM images of the fibers shown in figures 6(A)-g and h. Cell aspect ratio measurements demonstrated that overall, human tenocytes had a higher percentage of elongation within the gripped TEND compared to the loose TEND ($p < 0.01$) (figure 6(B)). This is due to the higher degree of fiber alignment and tension within the gripped TEND (figure 6(C)), resembling gripping in surgical graft fixation. On the contrary, within loose TEND there was significant loss of fiber alignment due to the absence of tension (figure

6(C)). Although loss of fiber alignment was observed within loose samples, it was shown that annealed TEND was still significantly more aligned than the as-electrospun TEND after 14 d in culture (figure 6(C)) highlighting the importance of the annealing process.

3.6. Mechanical properties of cellularized and acellular annealed TEND

As annealing led to improved tensile, material and 'porosity' properties of TEND, only annealed TEND was used for the remaining *in vitro* studies. Gripped and loose TEND were seeded with human tenocytes to assess the effects of cells on their mechanical strength and physical properties. After 7 and 14 d in culture, the samples were pulled to failure in the direction of aligned fibers. Overall, after 7 or 14 d, all TEND in culture lost a significant amount of strength and modulus compared to the control groups ($p < 0.05$). However, gripped TEND was significantly stronger and stiffer than loose TEND regardless of the presence or absence of cells ($p < 0.05$) (figures 7(A) and (B)). TEND without cells was significantly stronger than TEND with cells when gripped for 7 d in culture ($p < 0.05$) (figure 7(A)). However, after 14 d, the mechanical strength of TEND was maintained in the presence of cells ($p < 0.05$) (figure 7(A)). Although TEND in culture showed lower peak stress and modulus, there were no significant changes in the amount of load they could withstand ($p > 0.05$) (figure 7(C)). As load remained consistent and the dimensions of TEND changed while in culture, all effects on the calculated mechanical properties can be attributed to the swollen cross section leading to an increased cross-sectional area. After 14 d in culture, loose TEND had significantly higher strain at break than the other conditions tested ($p < 0.05$). Overall, all TEND in culture had significantly higher strain at break than controls ($p < 0.05$) (figure 7(D)).



3.7. Tenogenic gene expression of mesenchymal stem cells (MSCs) on TEND

TEND was coated with PRP to simulate prospective clinical use as a biological delivery vehicle with patient-derived PRP or other blood-based products. Clinical grade human MSCs grown on PRP-coated TEND in both static and bioreactor cultures for 3 d showed statistically significant upregulation of collagen type I, collagen type III, and tenascin C genes compared to the same cells cultured on tissue culture plates alone or supplemented with BMP-12 to induce tenogenic differentiation (figure 8). This suggests upregulation of tendon-like matrix synthesis

and induction of tenogenic differentiation from cultured stem cells on TEND. Ki67 downregulation in stem cells grown on PRP-coated TEND further indicated that stem cells proliferation was reduced suggesting exiting of the cell-cycle due to lineage commitment.

3.8. Biocompatibility of TEND *in vivo*

As-electrospun and annealed TEND were implanted subcutaneously in rats to assess biocompatibility, cellular infiltration and remodeling between the groups with different porosities/bulk densities yet otherwise identical grafts. At 2, 4, 8, and 16 weeks TEND

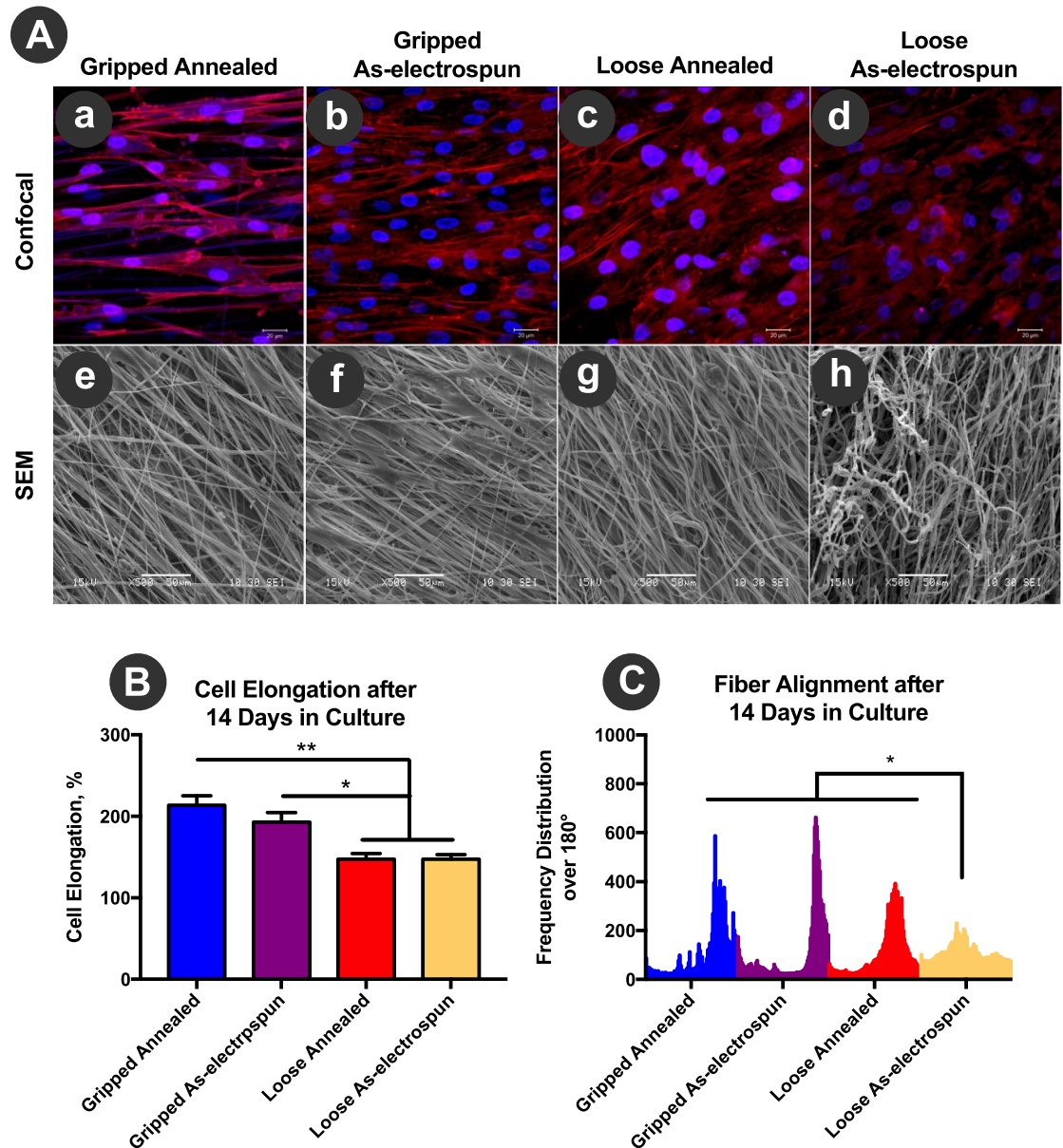
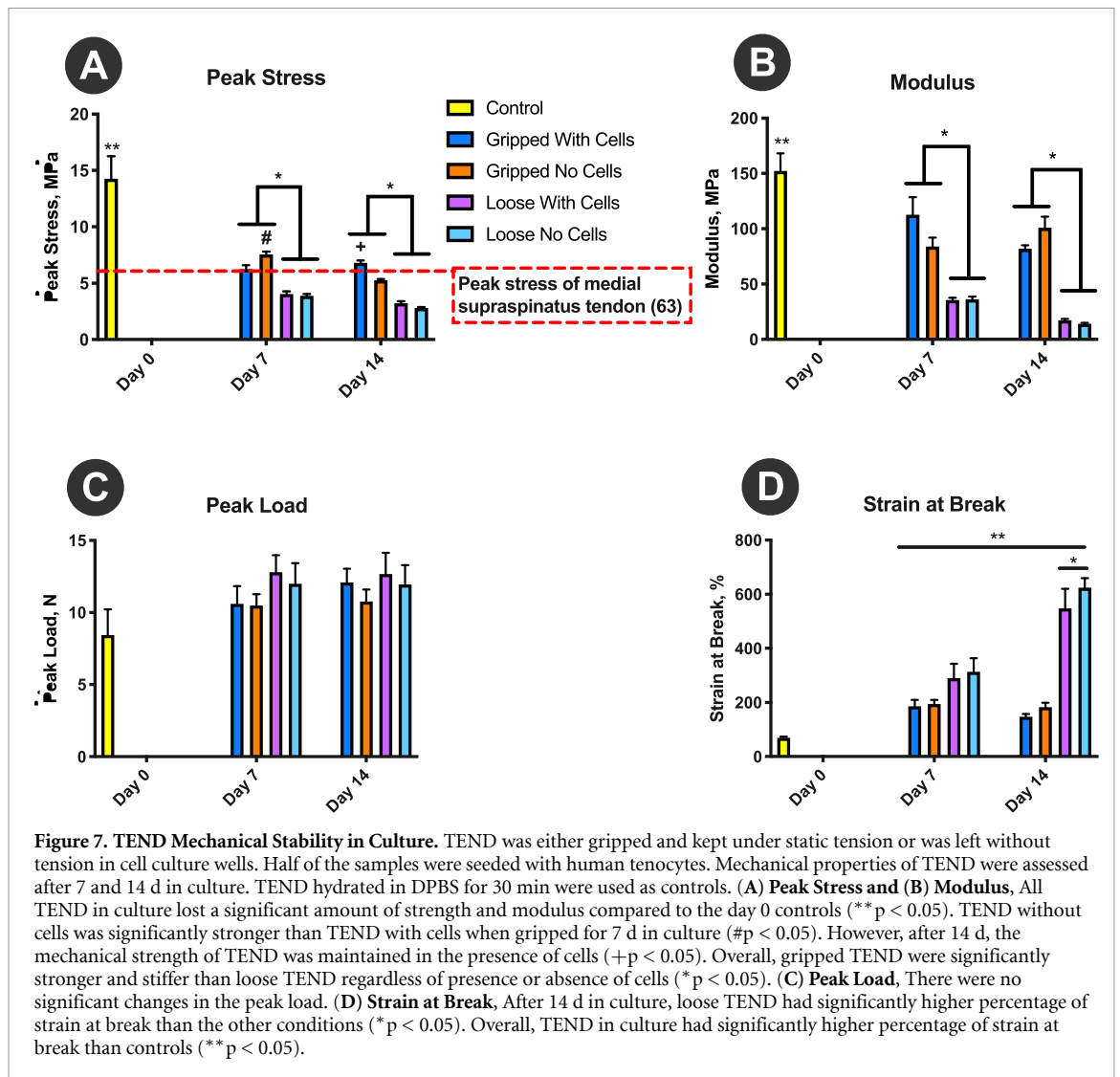


Figure 6. Cellular Elongation, Alignment, and Spreading on TEND. TEND was either gripped and kept under static tension or was left without tension in cell culture wells. All samples were seeded with human tenocytes and cellular spreading, elongation, and alignment was assessed after 14 d in culture. (A) **Cell Spreading**, gripped and loose TEND cultured with human tenocytes for up to 14 d were stained with DAPI nucleic stain (blue) and Alexa Fluor[®] 594 phalloidin actin filament stain (red), and imaged by confocal microscopy at 40x magnification. Scale bar = 20 μm. The direction of cell alignment does not match fiber direction in the SEM images as the images were taken using different microscopes and orientation. (B) **Cell Elongation**, both annealed and as-electrospun gripped TEND supported significantly higher percent cell elongation compared to the loose TEND (** $p < 0.0001$ and * $p < 0.01$). (C) **Fiber Alignment**, loose as-electrospun TEND significantly lost their fiber alignment compared to tensioned grafts after 14 d in culture (* $p < 0.0001$).

and decellularized human dermis were explanted, sectioned and stained with hematoxylin & eosin (H&E). Histology results and analyses of cell numbers within grafts at different time points showed that a higher number of cells infiltrated TEND in annealed groups compared to as-electrospun TEND (figure 9). Annealed TEND showed significantly higher cellular infiltration after 2 weeks (figure 9(B)). Allograft dermis exhibited an intense early inflammatory response at 2 weeks (figure 9(C)) with primarily mononuclear cells. Annealed TEND showed increased cellularization after 4 and 8 weeks (figures

9(E) and (H)) whereas allograft dermis progressed to fibrotic encapsulation shown at 8 weeks (figure 9(I)). Annealed TEND showed histological evidence of graft remodeling into dense host connective tissue by 16 weeks (figure 9(K)) while persistent fibrotic encapsulation was still present around allograft dermis (figure 9(L)).

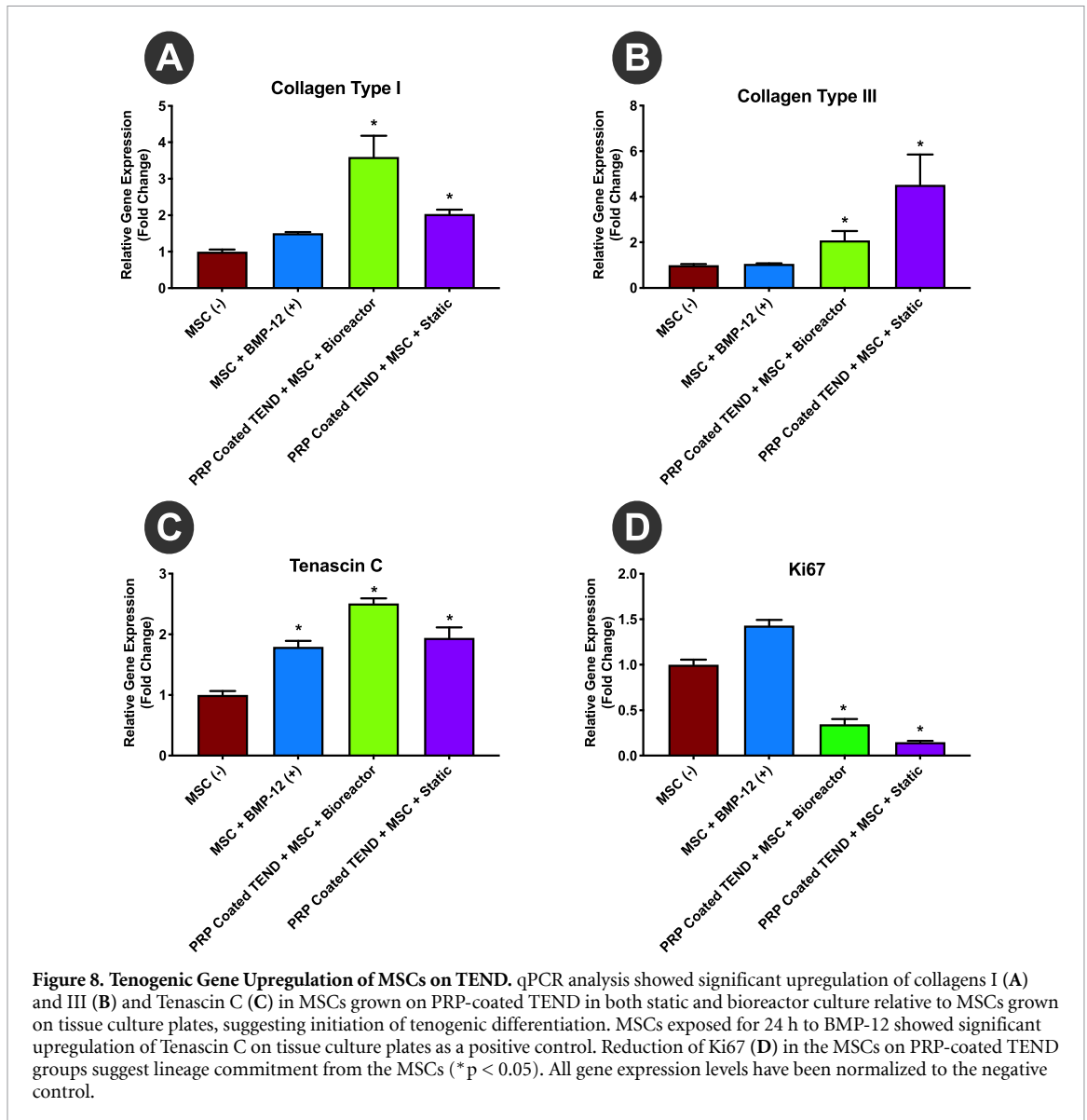
Annealed TEND was further tested in a clinically relevant tendon injury model by implantation around a Achilles tendon defect in rabbits (figure 10) to assess cellular infiltration, remodeling, and regeneration. TENDs were explanted at 16 and 52 weeks



and stained with H&E and Masson's trichrome. Histology images of suture only (sham) explants showed inflammatory cells at 16 weeks (figure 11(A)) and disorganized collagen formation (figures 11(B) and (C)). On the contrary, it was shown that annealed TEND was cellularized and started remodeling by 16 weeks (figures 11(D)–(F)). By 52 weeks, histology images indicate that TEND had fully remodeled and new collagen was formed. It was shown that the newly formed collagen in the sham group was randomly orientated (figures 11(G)–(I)) whereas highly organized, aligned collagen was formed within TEND (figures 11(J)–(L)). Collagen alignment was assessed by directionality function of ImageJ and it was shown that collagen formed in the presence of TEND, had significantly higher degree of alignment when compared to suture-only sham. This higher degree of alignment is denoted by the narrower width and higher peak of the histogram shown in figure 11(M).

3.9. Human cadaver surgical implantation of TEND in rotator cuff and achilles tendon

Current surgical repair of the ruptured Achilles tendon is performed through either an open approach (10–14 centimeter incision) or more commonly through a minimally invasive (3–4 centimeter incision) surgical technique in order to avoid the common postoperative wound complications. There are two commonly used grafts in the repair of Achilles tendons. Human decellularized cadaveric dermis and various forms of human preserved amniotic placental membrane. Both of these grafts have problems with implantation or fixation to the host tendon. Cadaver surgical implantation of TEND was performed with a minimally invasive technique that allowed easy graft orientation (colored fibers, figure 12) and delivery with its plastic inserter. TEND showed excellent handleability and suture fixation to the native tendon. These inherent characteristics of TEND should aid surgeons in clinical practice.



4. Discussion

In a bioinspired design based on the orderly linear anatomy of ligaments and tendons [8, 10], and with clinical translation in mind, we have developed a collagen-based electrospun TEND for the repair of musculoskeletal tissues. Electrospinning is a widely used method for the production of aligned microfibrillar constructs that can exhibit matrix structures analogous to the tendon ECM [11, 12, 52]. However, partly due to the usage of harmful solvents, poor cellular infiltration, use of non-clinical grade polymers and lack of standards for fiber characterizations to more clearly define product critical quality attributes [53], electrospun constructs have not been FDA approved or cleared as surgical mesh medical devices for ligament or tendon repair [17, 54]. This work shows significant progress towards overcoming these challenges. Designed for future clinical translation and human use, we have

pioneered an electrospinning process that allows scalable generation of collagen-based microfibrillar constructs for tendon and ligament tissue repair using a biologically benign solvent. This process combined with thermal annealing generates a biomaterial highly absorbent of blood and PRP with improved porosity and mechanical properties compared to conventionally electrospun grafts, overcoming major challenges inherent to clinical scale biomanufacturing via electrospinning.

Hybrid pneumatospinning-electrospinning allows the electrospinning of collagen and a wide array of possible stabilizing co-polymers, in particular PDLLA, from a benign solvent. This process has enabled us to engineer stable, strong, electrospun collagen-based constructs for tendon regeneration, while eliminating the use of toxic solvents. We further developed electrospinning and post-processing techniques to sufficiently remove residual solvent and improve stability in culture. Fiber diameters were

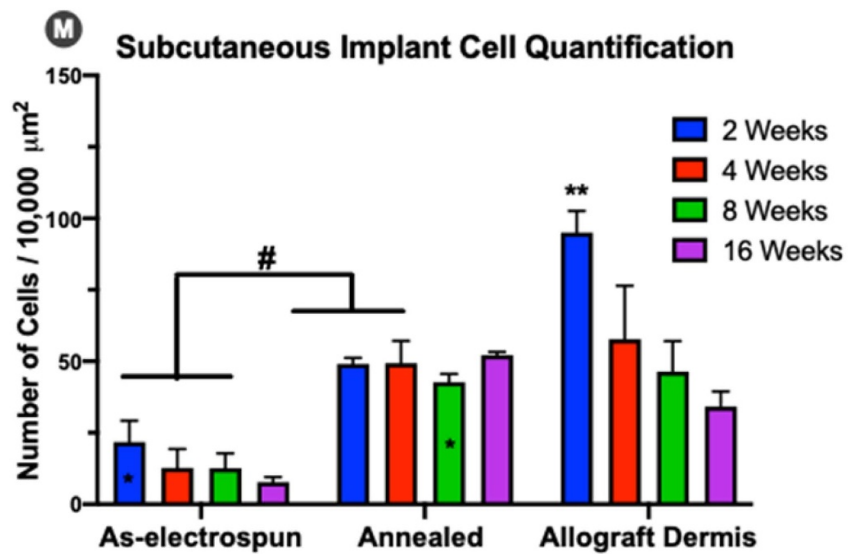
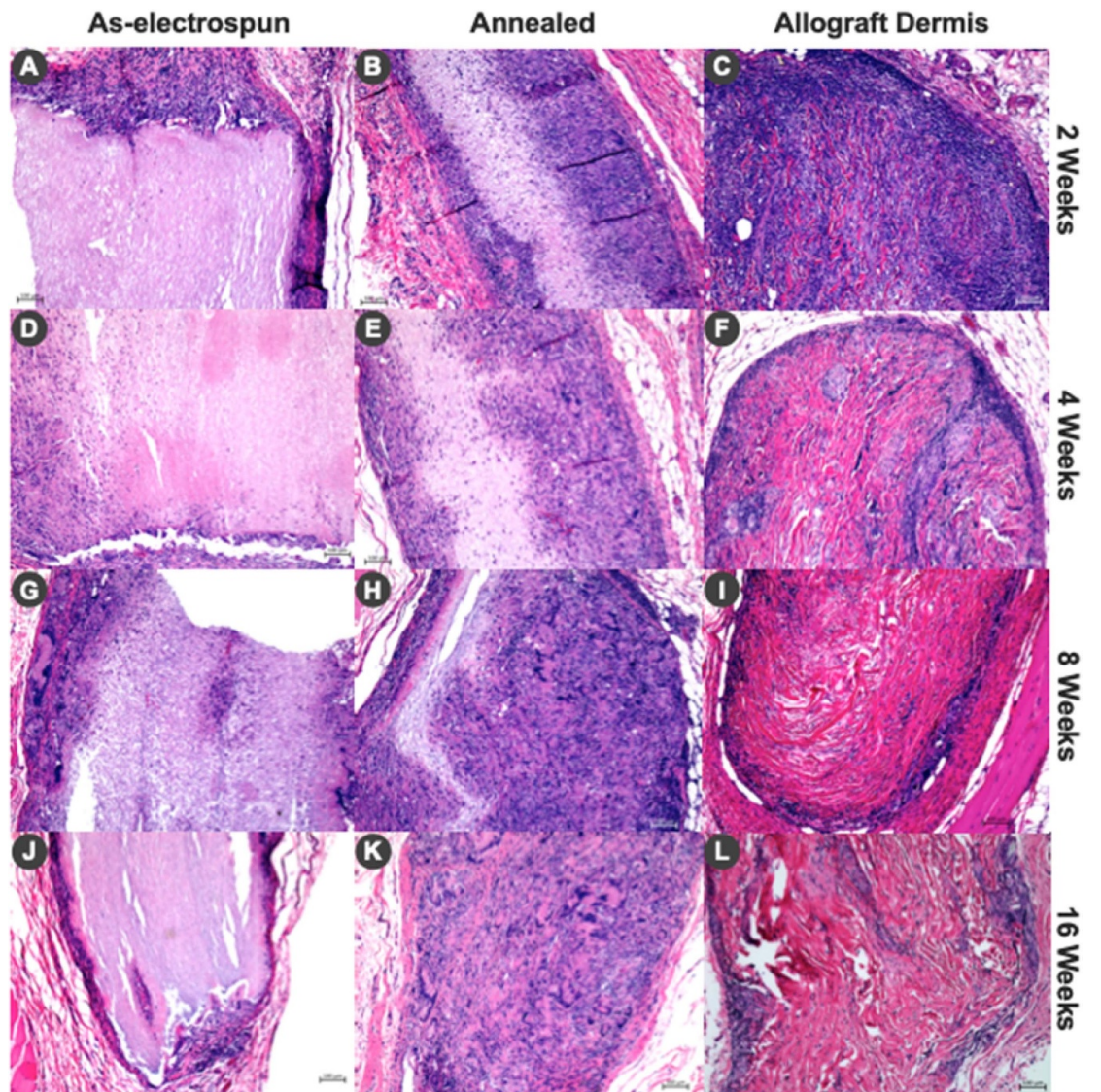


Figure 9. Histological Cellular Progression of TEND and Allograft dermis. Cellular infiltration through grafts after 2, 4, 8 and 16 weeks. (A)-(L) Histology sections of as-electrospun TEND, annealed TEND, and allograft dermis explanted at different time points. At 16 weeks, annealed TEND was fully infiltrated with cells and had some indication of remodeling as seen with change in eosin stain compared to allograft dermis. (M) Annealed TEND at all time points had significantly higher number of cells compared to the as-electrospun TEND (# $p < 0.05$) except the 8 weeks annealed TEND was not significantly different from the 2 weeks as-electrospun TEND (marked as *). Number of cells in allograft dermis at 2 weeks was significantly higher than the 8 and 16-weeks, annealed TEND at 2, 4 and 8-weeks, as well as the as-electrospun TEND at all time points (** $p < 0.05$).

Exposed Achilles Tendon



Full Thickness Incision

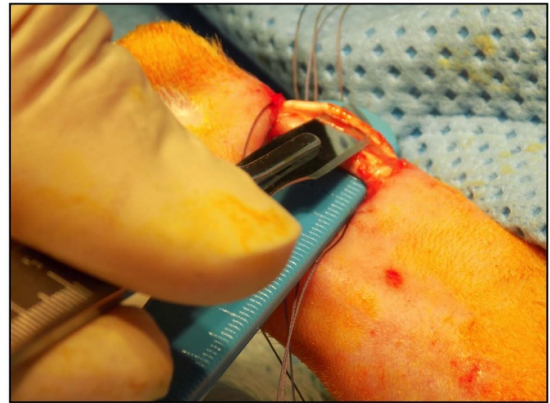


Figure 10. Tendon Injury Model Tested in Rabbits. TEND grafts were tested *in vivo* in the Achilles tendon of male New Zealand White Rabbits. To create the injury model prior to TEND implantation the calcaneal tendon was exposed through paratendineal incision of the cutis, subcutis and fascia. Three full thickness incisions (1 incision per bundle) approximately 7 mm long were made in the coronal plane of the Achilles tendon, midsubstance between the calcaneus and the gastrocnemius.

significantly smaller in annealed vs. as-electrospun TEND, likely related to the mechanical drawing forces imparted to the graft, which may have contributed to the stability and retained alignment upon hydration. Fiber diameter engineered into TEND may further be important for tendon repair in that electrospun microfibers larger than one micron, as found in TEND, have previously [55] been reported to upregulate mature tendon genes and tendon extracellular matrix production from human rotator cuff-derived cells.

Additionally, we showed that the internal void fraction of as-electrospun TEND can be significantly increased by low-temperature thermal annealing, as a putative mechanism for improved *in vivo* graft performance. As-electrospun TEND exhibited 7 μm diameter pores compared to over 100 μm pores in annealed TEND. This is significant when the average diameter of a mesenchymal cell at $\sim 35 \mu\text{m}$ is considered, and may directly relate to limitations of conventionally electrospun implants showing typical poor cell infiltration *in vivo* [16, 17] rather than a direct function of electrospun fiber size as previously believed [56, 57]. Post-processing of electrospun materials by thermal annealing is thus a robust, simple, scalable method whereby electrospun grafts can be biomanufactured to improve cellular infiltration potential, presenting a marked advancement for improving porosity or void-fraction within a fiber-based tissue engineered medical product (TEMP). Thermal annealing of TEND further led to enhanced mechanical stability in culture while maintaining molecular alignment and crystallinity. Our results are in agreement with studies by Fu *et al* that demonstrated the annealing process increased crystallinity and stability of poly(glycolide-co-lactide) [58]. We postulate that this annealing approach is not unique to collagen/PDLLA, but will be effective in increasing

the average pore size distribution and improving tensile properties in other electrospun grafts using other biological and synthetic polymers as well under appropriate conditions.

In biochemical analyses, SDS-PAGE showed the presence of alpha, beta and gamma chains in TEND as in the starting material. Additionally, the absence of laddering effect below 117kDa confirms that the low-temperature annealing process performed under vacuum did not result in collagen molecular breakdown. Similarly, previous studies have shown that dehydrothermal crosslinking of collagen, which is performed at high temperatures (over 100 °C) under vacuum does not result in molecular breakdown of collagen [59, 60]. FTIR was used to confirm the presence of collagen amide bonds I and II in electrospun and annealed TEND. However, amide III could not be easily distinguished because PDLLA has the same FTIR fingerprint as collagen in that region. As residual processing solvents are an important consideration for manufacturing of medical devices intended for human use, we further tested for residual DMSO solvent in TEND and showed levels 1000 times below the suggested dose limit per USP < 467.

Additionally, we demonstrated TEND rapidly absorbed blood and PRP. This is important for implant preconditioning as blood and PRP have been used commonly as biologics for improving rotator cuff, Achilles, and other tendon repairs and are believed to improve clinical outcomes [61]. Moreover, TEND soaked with PRP demonstrated improved mechanical strength, and also released growth factors present in PRP over two weeks at doses five times higher than native tendon tissue's release kinetics. Similar to our observations, Diaz-Gomez *et al* demonstrated increased stiffness of polycaprolactone nanofibers after coating with

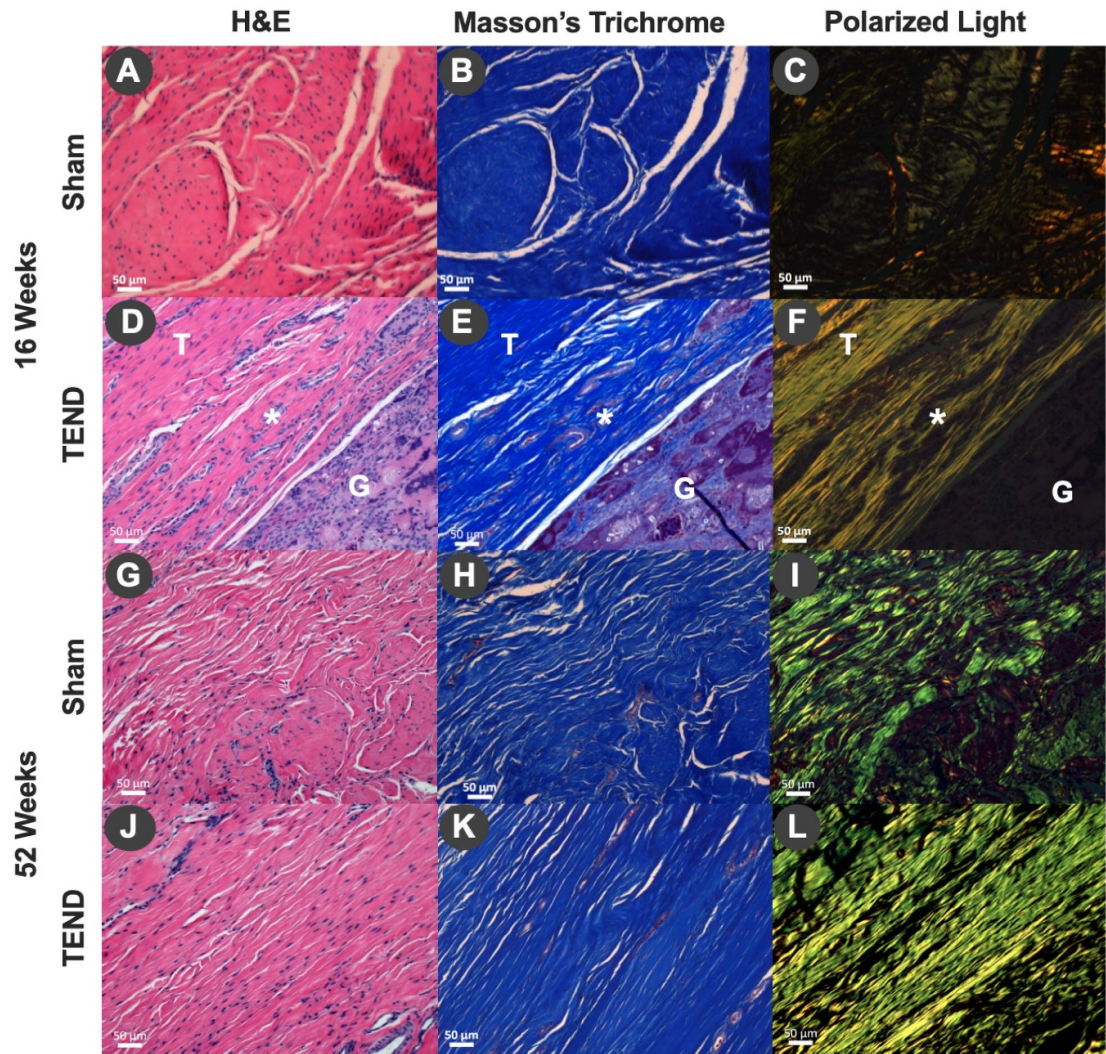


Figure 11. Rabbit Achilles Tendon Repair and Alignment of Newly Produced Collagen *In Vivo*. (A), (D), (G), (J) H&E and (B), (E), (H), (K) Masson's trichrome stains of sham and annealed TEND explanted at 16 and 52 weeks showed the progression of remodeling, from cell infiltration to collagen deposition. (C), (F), (I), (L) Polarized light microscopy showed an increase of aligned collagen fibers from 16 weeks to 52 weeks in the presence of TEND while the collagen fibers in sham were disorganized at 16 weeks as well as at 52 weeks. Tendon is denoted as T, TEND as G and Achilles tendon-graft interface where TEND has started remodeling as *. (M) Degree of collagen alignment and assessment of polarized light microscopy images of collagen produced *in vivo* 52 weeks after repairing rabbit Achilles tendons with or without TEND. It was shown that TEND promoted the deposition of collagen with significantly higher degree of alignment when compared to sham (* $p < 0.05$). This higher degree of alignment is denoted by narrower width and higher peak of the histogram.

PRP [62]. However, the mechanism of action resulting in higher stiffness of the PRP coated TEND needs further investigation. The higher growth factor

release kinetics observed in TEND compared to native tendon is resulted from higher absorption levels of PRP by TEND due to the higher surface area and

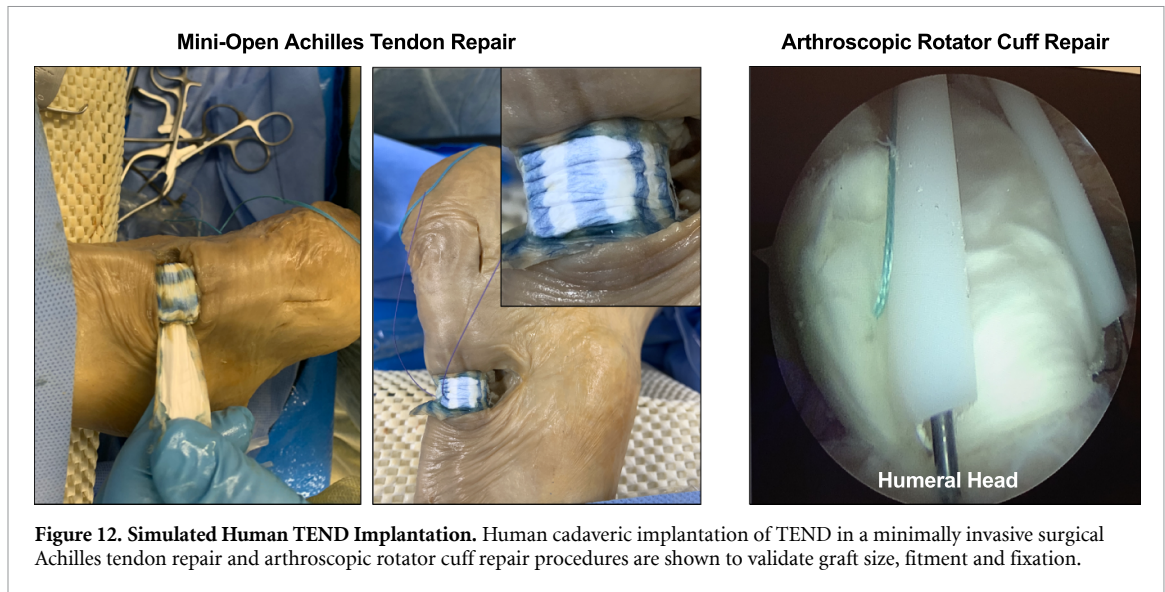


Figure 12. Simulated Human TEND Implantation. Human cadaveric implantation of TEND in a minimally invasive surgical Achilles tendon repair and arthroscopic rotator cuff repair procedures are shown to validate graft size, fitment and fixation.

porosity of TEND compared to native tendon. It is important to note that the release of growth factors from TEND at significantly higher levels compared to native tendon is crucial as these levels are comparable to the growth factor levels present in PRP when directly injected into the tendon repair site [63, 64]. High levels of PRP absorption and growth factor release by TEND and its mechanical strength suggest its suitability for ligament and tendon therapies as a carrier for these endogenous reparative factors.

As biological implants may be coated with PRP bedside, prior to implantation clinically, we tested the ability of our graft coated with PRP in the presence of stem cells in culture. PRP-coated TEND grown with clinical grade MSCs upregulated tenogenic differentiation markers and tendon-like extracellular matrix production. The expression of tenogenic genes is further significantly upregulated in TEND + PRP + MSCs cultured under cyclic loading in bioreactor cultures. Our results are in agreement with observations by Xu *et al* and Subramanian *et al*, which showed tenogenic differentiation of stem cells and upregulation of ECM under cyclic tensioning [65, 66]. This is significant in that TEND pretreated with patient blood or PRP, or implanted into a bleeding tendon or tendon-bone defect, can rapidly absorb growth factors present, which may together promote new tendon tissue formation *in vivo* as another possible tendon healing mechanism. The bioreactor culture used to cyclically load the graft may further be representative of simulating use (physical therapy) of the repaired tissue, which we showed to further improve tenogenic gene upregulation with MSCs grown on PRP-coated TEND. Additionally, the upregulation of collagens type I and type III may be important in tendon tissue engineering applications, as in natural tendon healing response, an increase in collagen type III synthesis followed by

higher proportions of collagen type I synthesis at later stages of healing is observed [67].

Cytocompatibility of anisotropic TEND was demonstrated through the attachment and organized morphology of human tendon cells. The results showed cellular elongation along the direction of aligned fibers within TEND. Cellular alignment is an intrinsic feature of native tendon and ligament tissue. Cellular alignment is shown to be imparted to cells grown on TEND by the structure-function relationship of the aligned substrate, which is not present in isotropic (disordered) matrices. Aligned fibers, as engineered into TEND, have previously been shown to promote tendon-like matrix synthesis, may mitigate adverse fibroblast (scarring) response [68] and is important for reducing the inflammatory immune response from unaligned fiber-based constructs [69]. Moreover, the organization of aligned fibers, as in TEND, is an important feature for promoting cellular alignment [70] with the secretion of extracellular matrix for *in vivo* tissue regeneration [71]. Fiber alignment is thus an important feature in a tendon-repair graft yet is an attribute missing in currently marketed medical devices such as acellular allograft dermis.

Simulating surgical fixation of a graft for use in tendon management, protection or augmentation, we further demonstrated that TEND gripped under tension, with or without cells, exhibited significantly higher strength over time compared to loose TEND. On average, the gripped TEND held upwards of 7.55 ± 0.6 MPa in peak stress and 83.9 ± 19.5 MPa modulus, after a 7-day culture. These tensile properties are comparable to the tensile properties of the middle (6.0 ± 2.6 MPa) and posterior (4.1 ± 1.3 MPa) portions of human supraspinatus tendons [72], further supporting the use of TEND in rotator cuff and other tendon injuries.

Moreover, annealed TEND exhibits marked improvements in *in vivo* cellular infiltration, which has been a pervasive challenge for traditionally electrospun materials [73–78]. Additionally, in a rabbit Achilles tendon injury model, developed based on studies by Van Kampen [51], TEND is shown to remodel by 52 weeks into dense, regularly oriented tendon-like tissue, showing an increased amount of tendon-like tissue growth, improved fiber alignment, and reduced tissue adhesions compared to surgical sham operated tendons. The cellular response to TEND *in vitro* and *in vivo* makes it an ideal biomaterial for a prospective clinical tendon repair graft where synthesis and conduction ('tenoconduction') of new, aligned dense collagen is needed to augment, regenerate or promote healing of the damaged tissue.

Finally, as TEND has been developed for and intended use in a clinically relevant medical device for tendon repair, handleability of this device during surgical implantation is of great importance. Therefore, in completion of TEND testing the handleability and surgical delivery of TEND was assessed in human cadaveric surgical implantation. TEND implanted with open, mini-open and minimally invasive techniques showed excellent handling, rapid and simple delivery and fixation to the native tendon, highlighting its applicability in clinical repair of tendon injury.

5. Conclusion

These studies provide the preclinical evidence on the suitability of TEND in safe and effective tendon repair and healing. Manufactured with benign solvents, clinical-grade materials and post-processing annealing, TEND exhibits near-native mechanical and material properties, cellular response and regenerative potential. This work overcomes current challenges in electrospinning for tendon and ligament repair by producing an aligned, collagen-based graft from benign solvents with high capacity to rapidly wick blood and other biological fluids, and cellular remodeling *in vivo*. These advancements allow for the biomaterial manufacturing of an anisotropic biomaterial with near-native mechanical strength. This biocompatible and cytocompatible device is promotive of *in situ* tissue remodeling, which may improve clinical outcomes in tendon and ligament repair indications.

Acknowledgments

This work was funded by the following organizations:

- The Defense Advanced Research Projects Agency (DARPA), grant HR0011-15-9-0006 (PI, MF).
- Commonwealth Research Commercialization Fund (CRCF), grant CP18-006 (PI, MF)
- The NIH, grant 1R43AR076841-01 (PI, MF)

All authors, except MR, BS, AB, KB, SA, and SBA were employed by Embody, Inc. We also thank Frank Reidy Research Center for Bioelectrics and Dr. Lesley Greene, Dr. John Cooper, and John Bedford at the ODU Chemistry Department for their help with chemical analyses. We thank Kevin Francis (<http://kfrancisdesigns.com/>) for designing graphics for figure 1.

Materials and Data Sharing

The biopolymer composition of TEND has been issued per US Patent 10,617,787. Method for producing TEND has been issued per US Patent 10,653,817.

ORCID iDs

Yas Maghdouri-White  <https://orcid.org/0000-0002-2010-2165>

Nardos Sori  <https://orcid.org/0000-0002-4561-6429>

Stella Petrova  <https://orcid.org/0000-0001-8621-1834>

Hilary Wriggers  <https://orcid.org/0000-0002-7987-774X>

Amrita Dasgupta  <https://orcid.org/0000-0002-4867-9476>

Kelly Coughenour  <https://orcid.org/0000-0003-2808-8887>

Michael P. Francis  <https://orcid.org/0000-0002-5551-9358>

References

- [1] Lui P P Y and Wong O T 2012 Tendon stem cells: experimental and clinical perspectives in tendon and tendon-bone junction repair *Muscles, Ligaments and Tendons. J.* **2** 163–8
- [2] Croy T, Saliba S, Saliba E, Anderson M W and Hertel J 2012 Differences in lateral ankle laxity measured via stress ultrasonography in individuals with chronic ankle instability, ankle sprain copers, and healthy individuals *J. Orthop. Sports Phys. Ther.* **42** 593–600
- [3] Kreitner K-F, Ferber A, Grebe P, Runkel M, Berger S and Thelen M 1999 Injuries of the lateral collateral ligaments of the ankle: assessment with MR imaging *Eur. Radiol.* **9** 519–24
- [4] Poehling G G, Curl W W, Lee C A, Ginn T A, Rushing J T, Naughton M J, Holden M B, Martin D F and Smith B P 2005 Analysis of outcomes of anterior cruciate ligament repair with 5-year follow-up: allograft versus autograft *Arthrosc. J. Arthrosc. Relat. Surg.* **21** 774.e1-774.e15
- [5] Snyder S J, Arnoczky S P, Bond J L and Dopirak R 2009 Histologic evaluation of a biopsy specimen obtained 3 months after rotator cuff augmentation with graftjacket matrix *Arthrosc. J. Arthrosc. Relat. Surg.* **25** 329–33
- [6] Lee D K 2007 Achilles tendon repair with acellular tissue graft augmentation in neglected ruptures *J. Foot Ankle Surg.* **46** 451–5
- [7] Aurora A, McCarron J, Iannotti J P and Derwin K 2007 Commercially available extracellular matrix materials for rotator cuff repairs: state of the art and future trends *J. Shoulder Elb. Surg.* **16** 171–8
- [8] O'Brien M 2005 The anatomy of the achilles tendon *Foot Ankle Clin.* **10** 225–38

- [9] Strickland S M, MacGillivray J D and Warren R F 2003 Anterior cruciate ligament reconstruction with allograft tendons *Orthop. Clin. North Am.* **34** 41–7
- [10] Lomas A J et al 2015 The past, present and future in scaffold-based tendon treatments *Adv. Drug Deliv. Rev.* **84** 257–77
- [11] Barber J G, Handorf A M, Allee T J and Li W J 2013 Braided nanofibrous scaffold for tendon and ligament tissue engineering *Tissue Eng. Part A* **19** 1265–74
- [12] Sheikh F A, Ju H W, Lee J M, Moon B M, Park H J, Lee O J, Kim J-H, Kim D-K and Park C H 2014 3D electrospun silk fibroin nanofibers for fabrication of artificial skin *J. Nanomed.* **11** 681–91
- [13] Jeong L, Lee K Y, Liu J W and Park W H 2006 Time-resolved structural investigation of regenerated silk fibroin nanofibers treated with solvent vapor *Int. J. Biol. Macromol.* **38** 140–4
- [14] Zhang C, Yuan H, Liu H, Chen X, Lu P and Zhu T et al 2015 Well-aligned chitosan-based ultrafine fibers committed teno-lineage differentiation of human induced pluripotent stem cells for Achilles tendon regeneration *Biomaterials* **53** 716–30
- [15] Yin Z, Chen X, Chen J L, Shen W L, Hieu Nguyen T M, Gao L and Ouyang H W 2010 The regulation of tendon stem cell differentiation by the alignment of nanofibers *Biomaterials* **31** 2163–75
- [16] Wang K, Zhu M, Li T, Zheng W, Li L, Xu M, Kong D and Wang L 2014 Improvement of cell infiltration in electrospun polycaprolactone scaffolds for the construction of vascular grafts *J. Biomed. Nanotechnol.* **10** 1588–98
- [17] Lannutti J, Reneker D, Ma T, Tomasko D and Farson D 2007 Electrospinning for tissue engineering scaffolds *Next Gener. Biomater.* **27** 504–9
- [18] Awad N K, Niu H, Ali U, Morsi Y S and Lin T 2018 Electrospun fibrous scaffolds for small-diameter blood vessels: A review *Membranes (Basel)* **8** 1–26
- [19] Wang X, Ding B and Li B 2013 Biomimetic electrospun nanofibrous structures for tissue engineering *Mater. Today* **16** 229–41
- [20] Sell S A, McClure M J, Garg K, Wolfe P S and Bowlin G L 2009 Electrospinning of collagen/biopolymers for regenerative medicine and cardiovascular tissue engineering *Nanofibers Regen. Med. Drug Deliv.* **61** 1007–19
- [21] Mano J F, Silva GA, Azevedo HS, Malafaya PB, Sousa RA and Silva SS et al 2007 Natural origin biodegradable systems in tissue engineering and regenerative medicine: present status and some moving trends *J. R. Soc. Interface* **4** 999–1030
- [22] Bürck J, Heissler S, Geckle U, Ardakani M F, Schneider R, Ulrich A S and Kazanci M 2013 Resemblance of electrospun collagen nanofibers to their native structure *Langmuir* **29** 1562–72
- [23] Pharmacology P M 2013 Clinical use of dimethyl sulfoxide (DMSO): a review *Int. J. Mol. Vet. Res.* **3** 23–33
- [24] Katsogiannis K A G, Vladislavljević G T and Georgiadou S 2015 Porous electrospun polycaprolactone (PCL) fibres by phase separation *Eur. Polym. J.* **69** 284–95
- [25] Jiang L, Wang L, Wang N, Gong S, Wang L, Li Q, Shen C and Turng L-S 2018 Fabrication of polycaprolactone electrospun fibers with different hierarchical structures mimicking collagen fibrils for tissue engineering scaffolds *Appl. Surf. Sci.* **427** 311–25
- [26] Lubasova D and Martinova L 2011 Controlled morphology of porous polyvinyl butyral nanofibers *J. Nanomater.* **2011** 6
- [27] Elamparathi A, Punnoose A M and Kuruvilla S 2016 Electrospun type 1 collagen matrices preserving native ultrastructure using benign binary solvent for cardiac tissue engineering *Artif. Cells Nanomed. Biotechnol.* **44** 1318–25
- [28] Sabantina Let al 2019 New polymers for needleless electrospinning from low-toxic solvents *Nanomaterials* **9** 52
- [29] Dong B, Arnoult O, Smith M E and Wnek G E 2009 Electrospinning of collagen nanofiber scaffolds from benign solvents *Macromol. Rapid Commun.* **30** 539–42
- [30] Hofman K, Tucker N, Stanger J, Staiger M, Marshall S and Hall B 2012 Effects of the molecular format of collagen on characteristics of electrospun fibres *J. Mater. Sci.* **47** 1148–55
- [31] Chen J L, Yin Z, Shen W L, Chen X, Heng B C, Zou X H and Ouyang H W 2010 Efficacy of hESC-MSCs in knitted silk-collagen scaffold for tendon tissue engineering and their roles *Biomaterials* **31** 9438–51
- [32] Sionkowska A 2011 Current research on the blends of natural and synthetic polymers as new biomaterials: review *Prog. Polym. Sci.* **36** 1254–76
- [33] He W, Yong T, Teo W E, Ma Z and Ramakrishna S 2005 Fabrication and endothelialization of collagen-blended biodegradable polymer nanofibers: potential vascular graft for blood vessel tissue engineering *Tissue Eng.* **11** 1574–88
- [34] Li X, Sanjeeva Murthy N and Latour R A 2012 The structure of hydrated poly (D, L - Lactic Acid) studied with x-ray diffraction and molecular simulation methods *Macromolecules* **45** 4896–906
- [35] Lin Y M, Boccaccini A R, Polak J M, Bishop A E and Maquet V 2006 Biocompatibility of poly-DL-lactic acid (PDLA) for lung tissue engineering *J. Biomater. Appl.* **21** 109–18
- [36] Hench L, Gautier S, Maquet V, Boccaccini A, Roether J and Jérôme R 2002 Development and in vitro characterisation of novel bioresorbable and bioactive composite materials based on polylactide foams and Bioglass® for tissue engineering applications *Biomaterials* **23** 3871–8
- [37] Maquet V, Boccaccini A R, Notingher I, Gough J E and Blaker J J 2003 In vitro evaluation of novel bioactive composites based on Bioglass®-filled polylactide foams for bone tissue engineering scaffolds *J. Biomed. Mater. Res. A* **67A** 1401–11
- [38] Pravata L, Boccaccini A R, Jérôme R, Maquet V and Notingher I 2003 Porous poly(α -hydroxyacid)/Bioglass® composite scaffolds for bone tissue engineering. I: preparation and in vitro characterisation *Biomaterials* **25** 4185–94
- [39] Polk S, Sori N, Thayer N, Kemper N, Maghdouri-White Y, Bulysheva A A and Francis M P 2018 Pneumatospinning of collagen microfibers from benign solvents *Biofabrication* **10** 045004
- [40] Liao S, Dong Y, Ramakrishna S, Chan C K and Ngiam M 2009 Degradation behaviors of electrospun resorbable polyester nanofibers *Tissue Eng. Part B* **15** 333–51
- [41] Srithep Y, Nealey P and Turng L-S 2013 Effects of annealing time and temperature on the crystallinity and heat resistance behavior of injection-molded poly(lactic acid) *Polym. Eng. Sci.* **53** 580–8
- [42] Weir N A, Buchanan F J, Orr J F, Farrar D F and Boyd A 2004 Processing, annealing and sterilisation of poly-L-lactide *Biomaterials* **25** 3939–49
- [43] Brown C, Zargar N, Abhari R E, Carr A and Mouthuy P-A 2016 Effect of annealing on the mechanical properties and the degradation of electrospun polydioxanone filaments *J. Mech. Behav. Biomed. Mater.* **67** 127–34
- [44] Ali S A M, Zhong S-P, Doherty P J and Williams D F 1993 Mechanisms of polymer degradation in implantable devices: I. Poly(caprolactone) *Biomaterials* **14** 648–56
- [45] Huisman E, Lu A, McCormack R G and Scott A 2014 Enhanced collagen type I synthesis by human tenocytes subjected to periodic in vitro mechanical stimulation *BMC Musculoskelet Disord.* **15** 386
- [46] Hou Y, Ni M, Lin S, Sun Y, Lin W, Liu Y, Wang H, He W, Li G and Xu L 2017 Tenomodulin highly expressing MSCs as a better cell source for tendon injury healing *Oncotarget* **8** 77424–35
- [47] Takahashi Y et al 2013 Tumor-derived tenascin-C promotes the epithelial-mesenchymal transition in colorectal cancer cells *Anticancer Res.* **33** 1927–34
- [48] Ballotta V 2014 Modulating the inflammatory response to biomaterials by mechanical stimuli: implications for in situ cardiovascular tissue engineering
- [49] Prihantono P, Hatta M, Binekada C, Sampepajung D, Haryasena H, Nelwan B, Asadul Islam A and Nilawati Usman A 2017 Ki-67 expression by immunohistochemistry

- and quantitative real-time polymerase chain reaction as predictor of clinical response to neoadjuvant chemotherapy in locally advanced breast cancer *J. Oncol.* **2017** 1–8
- [50] He X *et al* 2017 IFN- γ 1 regulates human dental pulp stem cells behavior via NF- κ B and MAPK signaling *Sci. Rep.* **7** 1–13
- [51] Van Kampen C, Arnoczky S, Parks P, Hackett E, Ruehlman D, Turner A and Schlegel T 2013 Tissue-engineered augmentation of a rotator cuff tendon using a reconstituted collagen scaffold: A histological evaluation in sheep *Muscles Ligaments Tendons J.* **3** 229–35
- [52] Wang Z, Lee W J, Koh B T H, Hong M, Wang W, Lim P N, Feng J, Park L S, Kim M and Thian E S 2018 Functional regeneration of tendons using scaffolds with physical anisotropy engineered via microarchitectural manipulation *Sci. Adv.* **4** 1–13
- [53] Garcia L, Soliman S, Francis MP, Yaszemski MJ, Doshi J and Simon JR CG *et al* 2019 Workshop on the characterization of fiber-based scaffolds: challenges, progress, and future directions *J. Biomed. Mater. Res. B* **108** 2063–72
- [54] Rogers J, Huang Y, Schmidt O G and Gracias D H 2016 Origami MEMS and NEMS *MRS Bull.* **41** 123–9
- [55] Erisken C, Zhang X, Moffat K L, Levine W N and Lu H H 2012 Scaffold fiber diameter regulates human tendon fibroblast growth and differentiation *Tissue Eng. Part A* **19** 519–28
- [56] Balguid A, Mol A, van Marion M H, Bank R A, Bouten C V C and Baaijens F P T 2008 Tailoring fiber diameter in electrospun poly(ϵ -Caprolactone) scaffolds for optimal cellular infiltration in cardiovascular tissue engineering *Tissue Eng. Part A* **15** 437–44
- [57] Rocco K A, Maxfield M W, Best C A, Dean E W and Breuer C K 2014 In vivo applications of electrospun tissue-engineered vascular grafts: a review *Tissue Eng. Part B* **20** 628–40
- [58] Fu B X, Hsiao B S, Chen G, Zhou J, Koyfman I, Jamiolkowski D D and Dormier E 2002 Structure and property studies of bioabsorbable poly(glycolide-co-lactide) fiber during processing and in vitro degradation *Polymer (Guildf)* **43** 5527–34
- [59] Cornwell K G, Pedro Lei S T and Andreadis G D P 2006 Crosslinking of discrete self-assembled collagen threads: effects on mechanical strength and cell–matrix interactions *J. Biomed. Mater. Res. A* **80A** 362–71
- [60] Drexler J W and Powell H M 2010 Dehydrothermal crosslinking of electrospun collagen *Tissue Eng. Part C* **17** 9–17
- [61] Hurley E T, Lim Fat D, Moran C J and Mullett H 2018 The efficacy of platelet-rich plasma and platelet-rich fibrin in arthroscopic rotator cuff repair: a meta-analysis of randomized controlled trials *Am. J. Sports Med.* **47** 753–61
- [62] Diaz-Gomez L, Alvarez-Lorenzo C, Concheiro A, Silva M, Dominguez F and Sheikh FA *et al* 2014 Biodegradable electrospun nanofibers coated with platelet-rich plasma for cell adhesion and proliferation *Mater. Sci. Eng. C* **40** 180–8
- [63] Lubkowska A, Dolegowska B and Banfi G 2012 Growth factor content in PRP and their applicability in medicine *J. Biol. Regul. Homeost. Agents* **26** 3–22
- [64] Kushida S, Kakudo N, Morimoto N, Hara T, Ogawa T, Mitsui T and Kusumoto K 2014 Platelet and growth factor concentrations in activated platelet-rich plasma: A comparison of seven commercial separation systems *J. Artif. Organs* **17** 186–92
- [65] Xu Y *et al* 2015 Cyclic tensile strain induces tenogenic differentiation of tendon-derived stem cells in bioreactor culture *Biomed. Res. Int.* **2015** 13
- [66] Subramanian G, Stasuk A, Elsaadany M and Yildirim-Ayan E 2017 Effect of uniaxial tensile cyclic loading regimes on matrix organization and tenogenic differentiation of adipose-derived stem cells encapsulated within 3D collagen scaffolds *Stem Cells Int.* **2017** 16
- [67] Sharma P and Maffulli N 2006 Biology of tendon injury: healing, modeling and remodeling *J. Musculoskelet Neuronal Interact.* **6** 181–90
- [68] Emanuele E, Visai L, Saino E, Cornaglia A I, Gualandi C, Imbriani M and Visai L 2011 Effect of electrospun fiber diameter and alignment on macrophage activation and secretion of proinflammatory cytokines and chemokines *Biomacromolecules* **12** 1900–11
- [69] Schoenenberger A D, Foolen J, Moor P, Silvan U and Snedeker J G 2018 Substrate fiber alignment mediates tendon cell response to inflammatory signaling *Acta Biomater.* **71** 306–17
- [70] Wagenhäuser M U, Pietschmann M F, Docheva D, Gülecüyüz M F, Jansson V and Müller P E 2015 Assessment of essential characteristics of two different scaffolds for tendon in situ regeneration *Knee Surg. Sport Traumatol. Arthrosc.* **23** 1239–46
- [71] Gigante A, Cesari E, Busilacchi A, Manzotti S, Kyriakidou K, Greco F, Primio R D and Mattioli-Belmonte M 2009 Collagen I membranes for tendon repair: effect of collagen fiber orientation on cell behavior *J. Orthop. Res.* **27** 826–32
- [72] Itoi E, Berglund L J, Grabowski J J, Schultz F M, Growney E S, Morrey B F and An K-N 1995 Tensile Properties of Supraspinatus Tendon *Orthop. Res. Soc.* **13** 578–84
- [73] Nathan A S, Mauck R L, Baker B M, Metter R B, Burdick J A, Gee A O and Mauck R L 2008 The potential to improve cell infiltration in composite fiber-aligned electrospun scaffolds by the selective removal of sacrificial fibers *Biomaterials* **29** 2348–58
- [74] Skotak M, Ragusa J, Gonzalez D and Subramanian A 2011 Improved cellular infiltration into nanofibrous electrospun cross-linked gelatin scaffolds templated with micrometer-sized polyethylene glycol fibers *Biomed. Mater.* **6** 55012
- [75] Soliman S, Sant S, Nichol J W, Khabiry M, Traversa E and Khademhosseini A 2011 Controlling the porosity of fibrous scaffolds by modulating the fiber diameter and packing density *J. Biomed. Mater. Res. A* **96A** 566–74
- [76] Nam J, Huang Y, Agarwal S and Lannutti J 2007 Improved Cellular Infiltration in Electrospun Fiber via Engineered Porosity *Tissue Eng.* **13** 2249–57
- [77] Formica F A, Öztürk E, Hess S C, Stark W J, Maniura-Weber K, Rottmar M and Zenobi-Wong M 2016 A bioinspired ultraporous nanofiber-hydrogel mimic of the cartilage extracellular matrix *Adv. Healthc. Mater.* **5** 3129–38
- [78] Leong M F, Rasheed M Z, Lim T C and Chian K S 2009 In vitro cell infiltration and in vivo cell infiltration and vascularization in a fibrous, highly porous poly(D,L-lactide) scaffold fabricated by cryogenic electrospinning technique *J. Biomed. Mater. Res. Part A* **91A** 231–40